

Contents

1 Problem Definition	3
1.1 Engineering Problem	3
1.2 Engineering Requirements (Functions, Objectives and Constraints)	3
2 Individual Designs	5
2.1 Introduction	5
2.2 Individual Design Specification	5
2.3 Proposed Design and Selection Process.....	11
3 Material Analysis and Selection	15
3.1 Preliminary Calculations	15
3.2 Relevant Material Constraints.....	15
3.3 Translation of Required FOCs and Derivation of Material Performance Indexes (MPIs)	16
3.4 Material Selection Process	19
5 Manufacturing Method Analysis and Selection.....	26
5.1 Translation of Design Requirements and Screening Process.....	26
6 Design Sustainability	32
6.1 Analysis of Sustainability Results	34
8 Appendix	35
8.1 References	35
8.2 MATLAB Code.....	37

1 Problem Definition

1.1 Engineering Problem

The aim is to develop an implantable ventricular assist device that is intended to assist hearts failing from cardiovascular diseases. This is for the company, VADInc. The device should pump blood at a sufficient pressure and flow rate to meet the body's needs. The target market would be mainly those that suffer from coronary artery disease. The economic viability of the device will be a key measure of success.

1.2 Engineering Requirements (Functions, Objectives and Constraints)

Functions:

The primary and secondary functions for the impeller pump will be stated here:

Primary Functions	Secondary Functions
Must ensure blood is pumped at a sufficient pressure and flow rate around the body.	Should ensure materials used are biocompatible.
Must ensure pressure exerted by the left ventricle is reduced/ less work.	The LVADs should also boost the start-up commercially and attract investors.
Must ensure the left ventricle is assisted for long periods of time.	Decrease the number of surgeries needed regarding coronary artery diseases.
Should ensure haemolysis is minimised/prevented.	

Objectives:

Objectives list, a pairwise comparison and an objective tree can be seen below:

Objectives	Justification
Safe	This is a device that will be implanted within the body. It is imperative the impeller is safe and should be the main objective. Safety should be maximised.
Durable	The impeller will be continuously operating therefore should resist continuous impact for a minimum of 5 years [1].
Cost Effective	Cost should be minimised as VADInc have a limited budget and will assess economic viability throughout its life cycle.
Eco-Friendly	Environmental impact should be minimised throughout the life cycle of the impeller.
Compact Efficiency	Mass should be limited for the given size constraints provided. Some users are within the 70+ age region where this objective is vital.
Operational Efficiency	An impeller that ensures efficient transfer of blood at a sufficient pressure and flow rate will assist the target market in keeping alive, with 80-85% alive a year after LVAD use thus far [1.2].

Objectives	Safe	Durable	Cost Effective	Eco-friendly	Compact Efficiency	Operational Efficiency	Total
Safe	-	1	1	1	1	1	5
Durable	0	-	0	1	0	1	2
Cost Effective	0	1	-	1	1	0	3
Eco-friendly	0	0	0	-	0	0	0
Compact Efficiency	0	1	0	1	-	1	3
Operational Efficiency	0	0	1	1	0	-	2

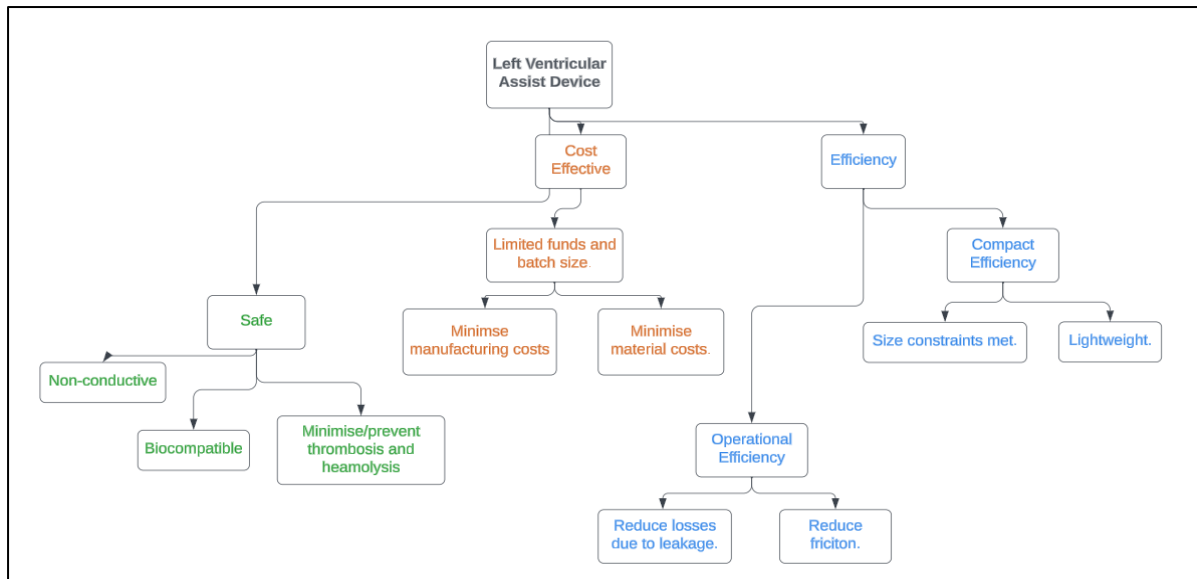


Figure 1.1: Objective tree for the LVAD.

Constraints:

The following design limitations imposed for the development of the device are the following:

Constraints
Must fit within a casing of 100 mm diameter.
Device's pump must achieve a volumetric flow rate of water of 75litre/min against a pressure difference of 0.80 bar .
Constraints related to material choice [Section 3].
Inlet blade height is to be between 0.004m and 0.020m .
Outlet blade height is to be between 0.004m and 0.008m .
Angle Outflow Dislaign should not exceed 1.5° .

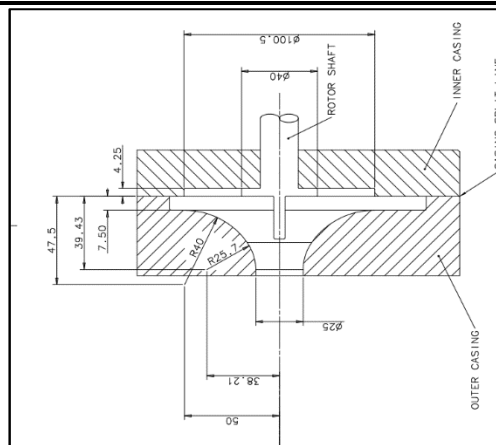


Figure 1.2: Casing for the LVAD impeller

2 Individual Designs

2.1 Introduction

The impeller required here would be cased within a centrifugal micropump as the impeller draws fluid into the pump and exits the pump at an outlet velocity that is higher to ensure blood flows around the body at a sufficient flow rate and pressure. This section will be based on impeller designs for this process, one of an operating speed of 2300rpm as well as the final impeller operating at a speed of 2600rpm.

The impellers designed must ensure certain constraints are met in addition to [Table 1.3](#):

- Inlet blade height [b_1]: $0.004\text{m} < b_1 < 0.020\text{m}$
- Outlet blade height [b_2]: $0.004\text{m} < b_2 < 0.008\text{m}$

2.2 Individual Design Specification

The key parameters of the impeller will be detailed with these being velocity mismatch, angle outflow disalign and the blockage factors:

Outflow Angle Misalignment:

This is the difference between the outlet flow angle and the volute spiral angle:

$$\alpha_{\text{Outflow Disalign}} = \alpha_s(\text{Volute spiral angle}) - \alpha_2(\text{Outlet flow angle}) \quad (2.1)$$

This parameter is significant as keeping the disalign as small as possible ensures the absolute velocity at the impeller travels in a direction that is as close to the spiral of the volute as possible. This ensures a smooth transition and prevent minimise flow disturbances, arising shear stress and so damaging the blood cells.

Velocity Mismatch:

This is the difference between the velocity at the diffuser entry and the absolute velocity at the exit of the impeller:

$$v_{\text{Differenec(Mismatch)}} = \left(\sqrt{v_{2,n}^2 + v_{2,t}^2} - \frac{Q_{\text{Required flow rate}}}{A_{\text{Diffuser area}}} \right) \quad (2.2)$$

The component $\sqrt{v_{2,n}^2 + v_{2,t}^2}$ refers to the absolute value of the exit velocity and $\frac{Q_{\text{Required flow rate}}}{A_{\text{Diffuser area}}}$ being the velocity at the diffuser entry. Checking this parameter is vital, to ensure there is no sudden jump in velocity which would otherwise cause for the formation of vortices and so ultimately reduce efficiency.

Blockage Factors and Number of Blades:

There are 2 blockage factors that must be considered, one at the inlet and one at the outlet. This considers the flow section taken up due to the presence of the impeller blades:

$$B_{f1,2} = \frac{A_{1,2} - A_{b1,2}}{A_{1,2}} \text{ where 1 indicates inlet and 2 the outlet} \quad (2.3)$$

Increasing this means that less obstruction to the blood flow in this case of the VAD which could lead to more efficient flow. This would also decrease the chance of possible clot formation and so for this case a lower blockage factor is desirable.

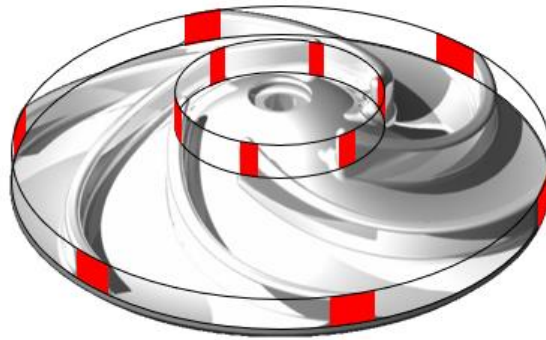


Figure 2.1: Blockage factor schematic. Red areas show blockage from impeller blade.

Parameters for the individual design has been chosen to ensure these key parameters where limited however compromises also had to be made which will be detailed later in the report.

Calculations for impeller design:

The calculations related to deriving performance parameters such as those are detailed below. A list of the known design variables is shown below for convenience:

Design Parameters	Notation
Operating Speed [rpm]	ω
Inner Radius [m]	r_1
Outer Radius [m]	r_2
Inlet Blade Height [m]	b_1
Outlet Blade Height [m]	b_2
Inlet Blade Thickness [m]	t_1
Outlet Blade Thickness [m]	t_2
Leading Edge Angle [degrees]	β_1
Trailing Edge Angle [degrees]	β_2
Number of Blades	n
Volute Spiral Angle	α_s

Figure 2.2: Impeller design parameters

The flow rate and pressure rise constraints had been modified initially to consider losses. A 20% increase in the flow rate was used to account for losses and a 40% increase in the pressure rise for losses:

$$Q_{old} = 75 \text{ litres/min} = 1.25 \times 10^{-3} \text{ m}^3/\text{s}$$

$$Q_{new} = 1.25 \times 10^{-3} \text{ m}^3/\text{s} \times 1.2 = 1.5 \times 10^{-3} \text{ m}^3/\text{s}$$

$$\Delta P_{new} = 0.8 \times 1.4 = 1.12 \text{ bar}$$

The water horsepower and brake horsepower were considered equal when assuming no losses. This allowed for the required power of the impeller to be calculated:

$$whp = bhp = Q_{new} \times \Delta P_{new} = 168 \text{ W} \quad (2.4)$$

The equation for the net head is as follows but is simplified by assuming radial inlet flow. The term $\omega r_1 v_{1,t}$ would be 0 due to the inlet tangential velocity $[v_{1,t}]$ being 0:

$$H = \frac{1}{g} (\omega r_2 v_{2,t} - \omega r_1 v_{1,t}) \quad (2.5)$$

Assuming no tangential inlet flow leads to the flow rate of the fluid being equal to the following:

$$Q = 2\pi b_1 \omega r_1^2 \tan \beta_1 \quad (2.6)$$

This assumption means that the impeller consists of only radial inlet flow. Using [equation 2.5](#), the leading-edge angle of the impeller is as follows:

$$\beta_1 = \arctan \left(\frac{Q_{new}}{2\pi b_1 \omega r_1^2} \right) \quad (2.7)$$

However, the blockage factor does need to be considered and would affect the flow rate due to obstructed flow leading to a leading-edge value of:

$$\beta_1 = \arctan \left(\frac{Q_{new}}{2\pi b_1 B_{f1} \omega r_1^2} \right) \quad (2.8)$$

The trailing edge can be calculated as shown below. It must be stated that the outlet tangential velocity $[v_{2,t}]$ is NOT 0 as only $v_{1,t}$:

$$\beta_2 = \arctan \left(\frac{v_{2,n}}{\omega r_2 - v_{2,t}} \right) \quad (2.9)$$

The outlet tangential and normal velocities $[v_{2,t} \text{ and } v_{2,n}]$ can be calculated as follows. The assumption of inlet radial flow, allows for a simplified equation for the tangential outlet velocity:

$$v_{2,n} = \frac{Q_{new}}{2\pi r_2 b_2 B_{f2}} \text{ and } v_{2,t} = \frac{gH}{\omega r_2} \quad (2.10)$$

Finally, the angle between the rotor and absolute outlet velocity $[v_2]$ can be calculated:

$$\alpha_2 = \arctan \left(\frac{v_{2,n}}{v_{2,t}} \right) \quad (2.11)$$

Assuming inviscid flow leads to the assumption the flow further away from the blades are less effected by them. This is as viscous forces near the blade surface are neglected. Assuming that the flow is only tangential to the blades, means that a new lower tangential speed must be considered, $v'_{2,t}$. The slip factor is introduced and has the equations:

$$\sigma = \frac{v'_{2,t}}{v_{2,t}} = 1 - \frac{\sqrt{\sin(\beta)}}{n^{0.7}} \quad (2.12)$$

This also implies that the new angle from [equation 2.12](#), would be greater as $\frac{v_{2,n}}{v_{2,t}}$ is greater.

All the required equations have now been derived to calculate the parameters for different operating speeds.

Parameter values for individual design:

Using the calculations above and parameters in [figure 2.1](#), the parameters are as follows:

Design Paramters	Value
Number of Blades	6
Inner Radius (m)	0.017
Outer Radius (m)	0.05
Inlet Blade Height (m)	0.011
Outlet Blade Height (m)	0.006
Inlet Blade Thickness (m)	0.002
Outlet Blade Thickness (m)	0.002
Inlet Blockage Factor	0.72
Outlet Blockage Factor	0.88
Outlet Blockage Factor Mismatch	0
Inlet Blockage Factor Mismatch	0
Leading Edge Angle (degrees)	23.4
Trailing Edge Angle (degrees)	18.2
Velocity Mismatch (m/s)	2.47
Outflow Angle Disalign (degrees)	-1.3
Speed (rpm)	2300
Net Head (m)	11.42

Figure 2.3: Individual impeller design parameters.

Justification for geometrical parameter choice:

The **key dependent parameters** which are the angle outflow misalign, the velocity mismatch and the blockage factors will be analysed against the number of blades and the outlet blade height. The MATLAB code ensures a change in variables like the number of blades still means the guessed blockage factors is equal to the calculated each time:

Key dependent parameters vs Number of Blades:

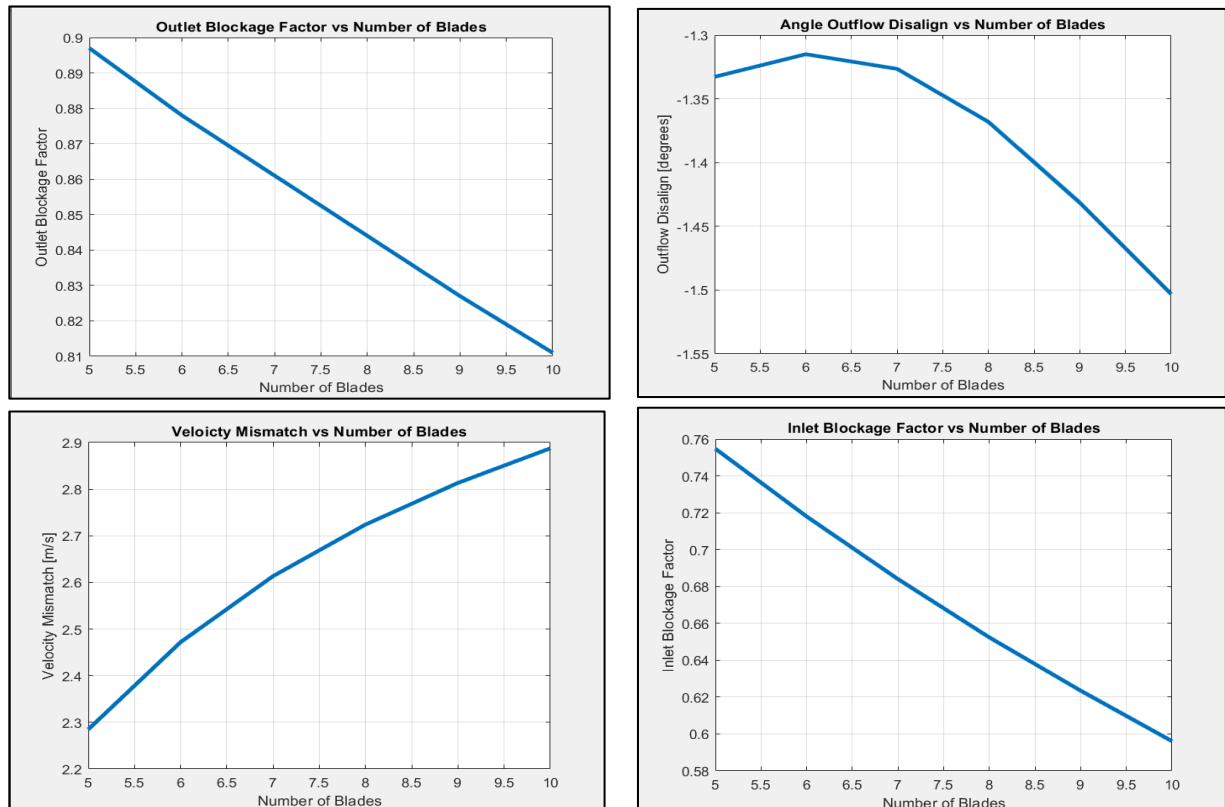


Figure 2.4,2.5,2.6 & 2.7: Graphs of the key dependent parameters against the number of blades.

The number of blades chosen is 6 whereby the graphs above show it is a suitable compromise. With the increase in the number of blades, the outlet and inlet blockage factors decrease which is not what is desired hence it was imperative that the number of values was kept to the lower end. This meant an outlet blockage factor of 0.88 and 0.72 was obtained with 6 blades which were both feasible values. The absolute value of the outflow misalign mainly increases with the increase in blade number however from 5 to 6 blades there is a decrease from 1.33° to 1.31° , therefore 6 blades providing the least outflow angle misalign. The velocity mismatch does increase with the number of blades again meaning lower blade numbers are preferred. However, since the difference between 5 and 6 blades is only 0.19m/s as well as the other points stated, **6 number of blades is the best compromise**. It is an **average** amount as well **preventing sever slip conditions and increased circulatory losses if too few and boundary layer growth if too much**.

Key dependent parameters vs Outlet Blade Height:

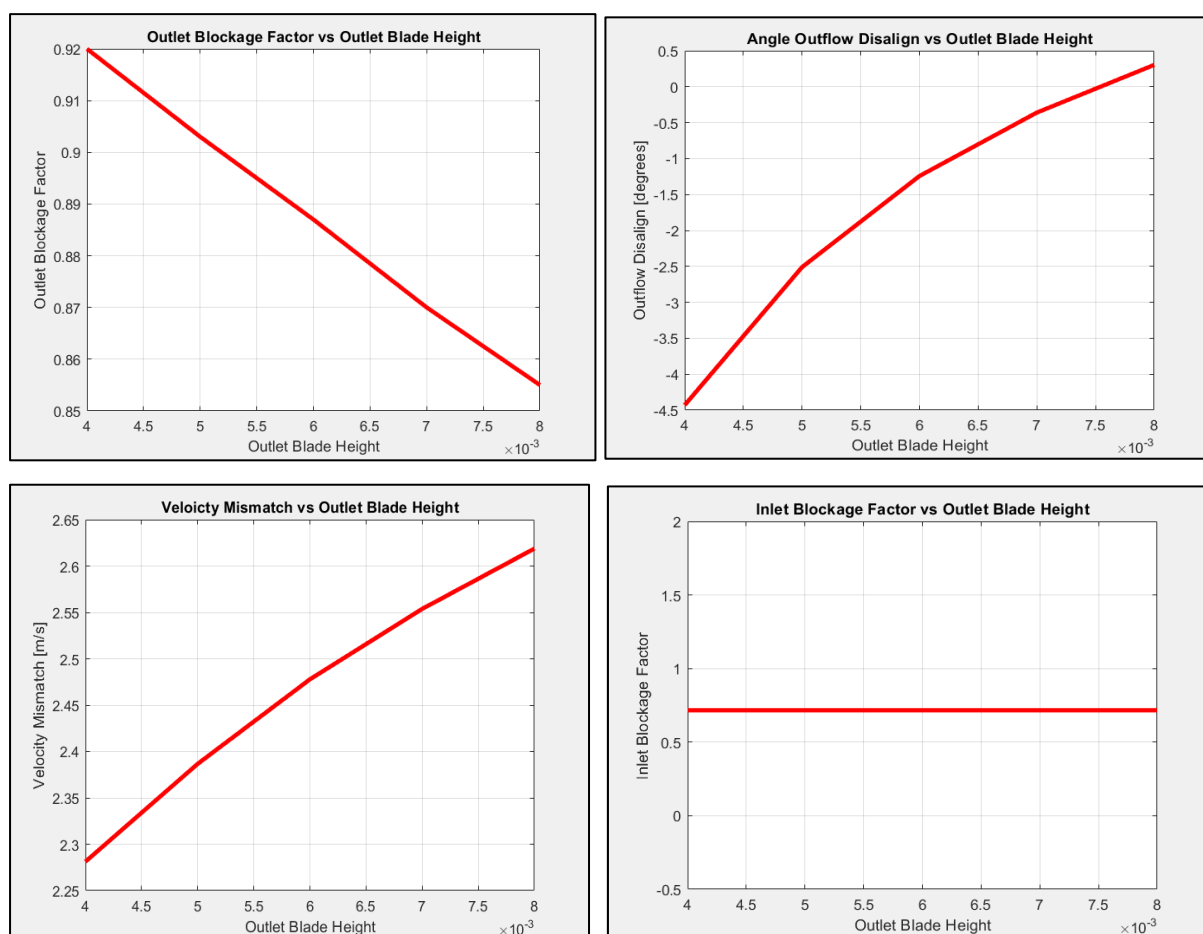


Figure 2.8,2.9,2.10 & 2.11: Graphs of the 4 key dependent parameters against the number of blades.

It should be noted the number of blades used here was 6 as well as the outlet blade height kept as 0.011m here. With an increase in the outlet blade height, a decrease in the outlet blockage factor can also be seen. The choice of a 0.006m outlet blade height still provides a high blockage factor of 0.88. This choice is viable as the outflow angle disalign exceeds 1.5° for any outlet blade height below 0.006m so **compromises between these 2 variables**. Velocity mismatch exceeds with a greater outlet blade height so choosing 0.006m satisfies the outflow constraint whilst minimising decrease in outlet blockage factor and increase in velocity mismatch. The inlet blockage factor is constant at 0.72 as expected due to inlet blockage factor being independent of outlet values.

CAD Drawings of Individual Design:

The CAD drawing of the individual design operating at 2300rpm along with its dimensions can be seen below:

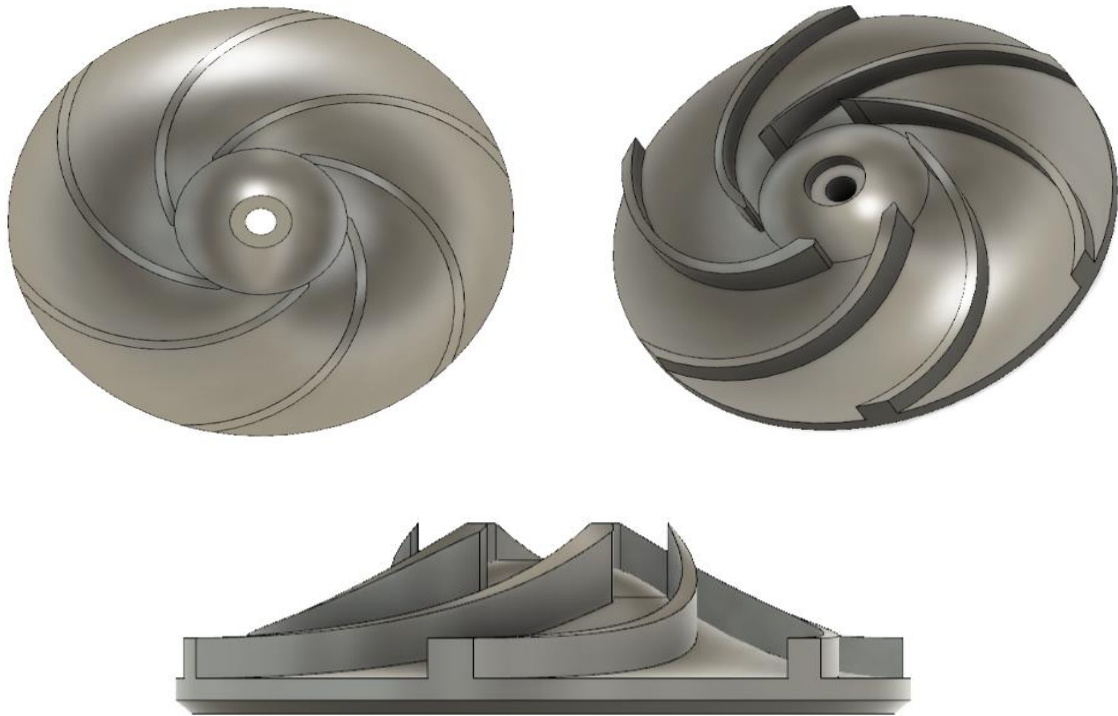


Figure 2.12, 2.13, 2.14: Top, front and cornered view of the impeller.

Dimensions including the inlet and outlet blade heights of the impeller can be seen below:

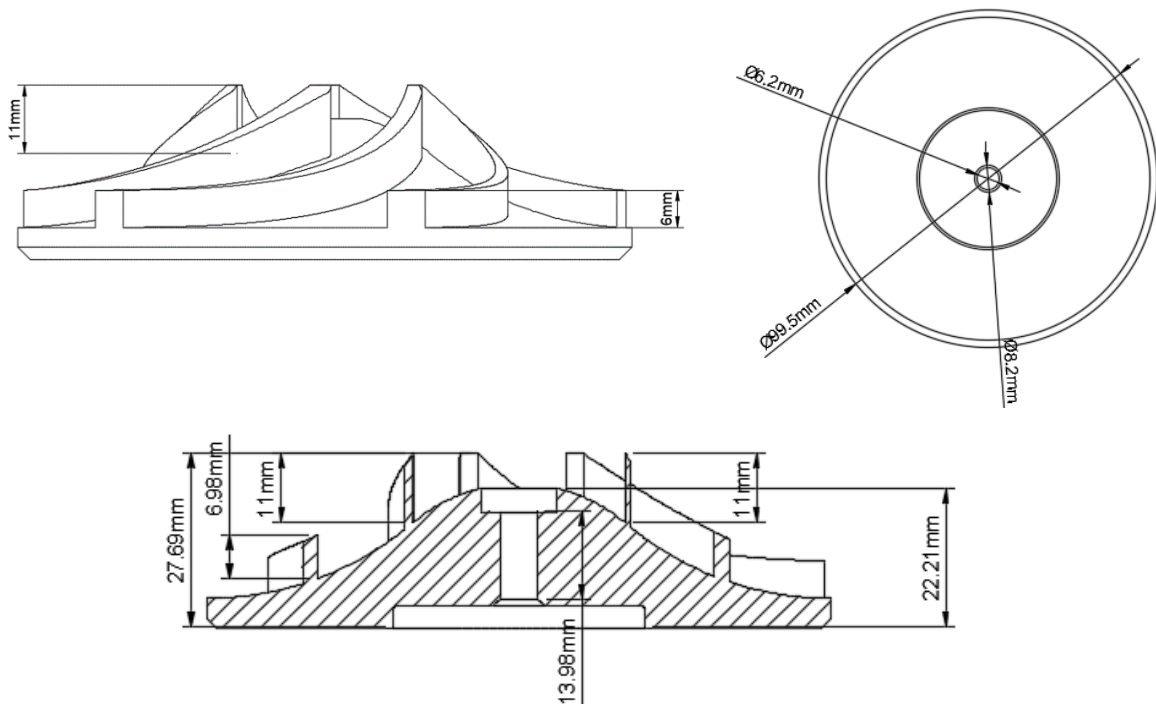


Figure 2.14, 2.15 & 2.15.2: Front and top view impeller dimensions

2.3 Proposed Design and Selection Process

With the key parameters now known, a pairwise comparison will again be used to rank these parameters by importance:

Key Parameters	Outflow Misalign [degrees]	Velocity Difference [m/s]	Inlet Blockage Factor	Outlet Blockage Factor	Score	Weighting
Outflow Disalign [degrees]	-	0	1	1	2	0.33
Velocity Mismatch [m/s]	1	-	1	1	3	0.5
Inlet Blockage Factor	0	0	-	0	0	0.01
Outlet Blockage Factor	0	0	1	-	1	0.16

Figure 2.16: Key parameter values for different operating speeds of the impeller.

Velocity mismatch is the most important parameter as the greater this is, the possibilities for blood cell damage arise because of hemolysis. Also, high velocity mismatches can cause high shear stress leading to thrombosis causing formation of blood clots. Outflow angle disalign is also important as ensuring blood flows in the correct direction as well as limitation of cavitation. The blockage factors were not weighed as heavily due to not as the other 2 variables would be more likely to cause the health issues stated before. The outlet was weighed as more important as there should be minimal obstruction to the blood exiting the impeller or else severe health complications could arise.

The key parameters including the inlet and outlet blockage factor, the velocity mismatch and outflow angle misalignment are shown below for each impeller made according to their respective operating speeds:

Key Parameters	Operating Speed (rpm)					
	2300	2400	2500	2600	2700	2800
Outflow Disalign [degrees]	-1.3	-1.16	-0.52	0.78	-1.36	-2.15
Velocity Mismatch [m/s]	2.47	2.19	2.07	1.83	1.9	3
Inlet Blockage Factor	0.72	0.66	0.9	0.75	0.81	0.45
Outlet Blockage Factor	0.88	0.8	0.81	0.76	0.94	0.49

Figure 2.17: Key parameter values for different operating speeds of the impeller.

With the values for the key parameters known, an evaluation scheme can now be used to rate these values. The rating for these values can be seen as follows:

Percentage	Rating
0-20%	Bad
21-40%	Weak
41-60%	Moderate
61-80%	Good
81-100%	Excellent

	Operating Speed (rpm)					
Key Parameters	2300	2400	2500	2600	2700	2800
Outflow Disalign [degrees]	60%	65%	80%	70%	55%	35%
Velocity Mismatch [m/s]	45%	55%	65%	85%	80%	35%
Inlet Blockage Factor	72%	65%	70%	75%	80%	40%
Outlet Blockage Factor	85%	80%	85%	80%	90%	45%

Figure 2.18: Evaluation percentages for values for different operating speeds of the impeller.

The weighting value for each key parameter will now be used to normalise the data from figure 2.17. This is done by multiplying the weighting for the key parameter by the associated percentages for each speed shown above:

	Operating Speed (rpm)					
Key Parameters	2300	2400	2500	2600	2700	2800
Outflow Disalign [degrees]	19.80%	21.45%	26.40%	23.10%	18.15%	11.55%
Velocity Mismatch [m/s]	22.50%	27.50%	32.50%	42.50%	40%	17.50%
Inlet Blockage Factor	0.72%	0.65%	0.70%	0.75%	0.80%	0.40%
Outlet Blockage Factor	13.60%	12.80%	13.60%	12.80%	14.40%	7.20%
Total	56.62%	62.40%	73.20%	79.15%	73.35%	36.65%

Figure 2.19: Normalised data with speed of 2600rpm having the highest total score.

The results show that the impeller made to run under an operating speed of 2600 rpm is the best choice and do this was then chosen as the final design.

CAD Drawings of Chosen Design:

The CAD drawing of the individual design operating at 2300rpm along with its dimensions can be seen below:

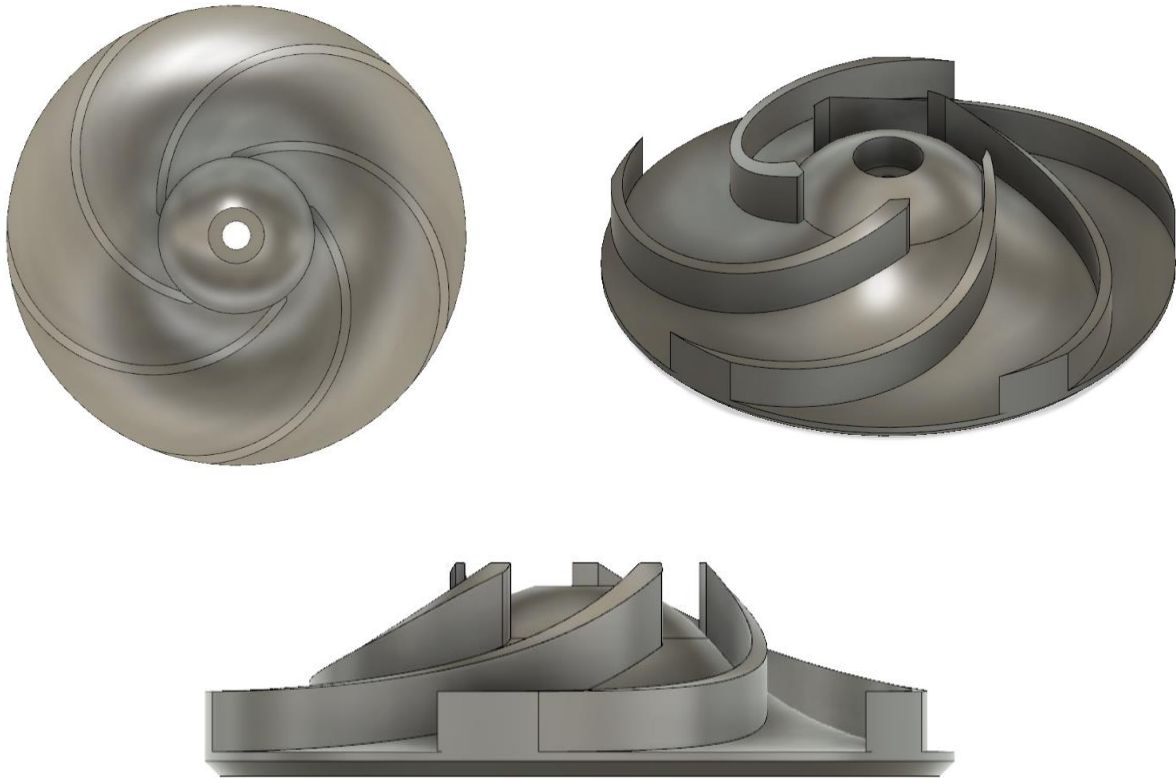


Figure 2.20, 2.21, 2.22: Top, front and cornered view of the chosen impeller.

Rendered versions of the final impeller are seen below:

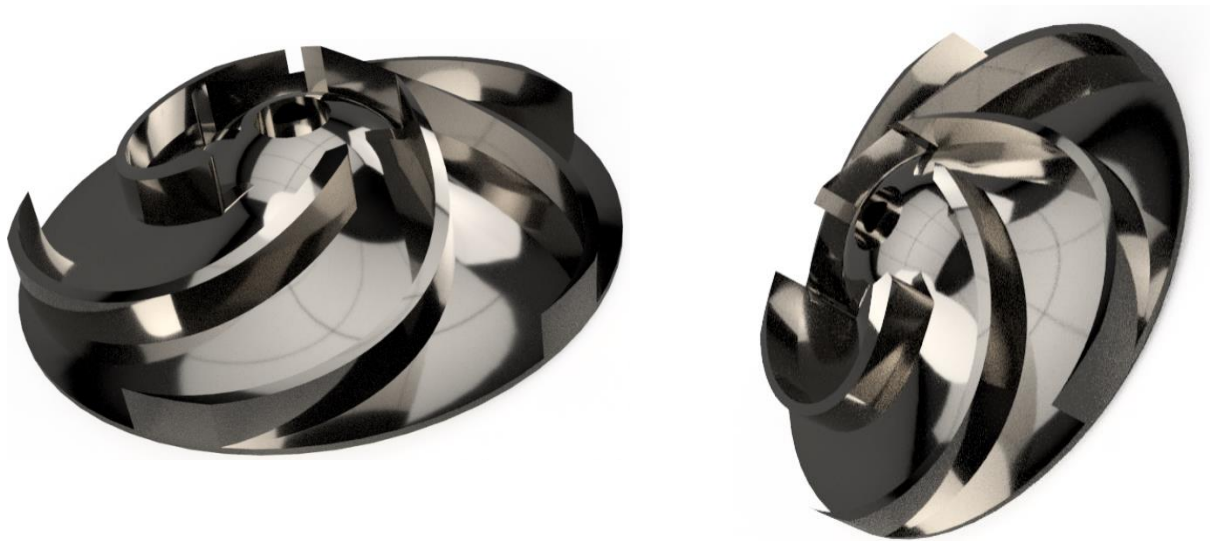


Figure 2.23, 2.24: Rendered designs of chosen impeller.

The dimensions drawings are as follows:

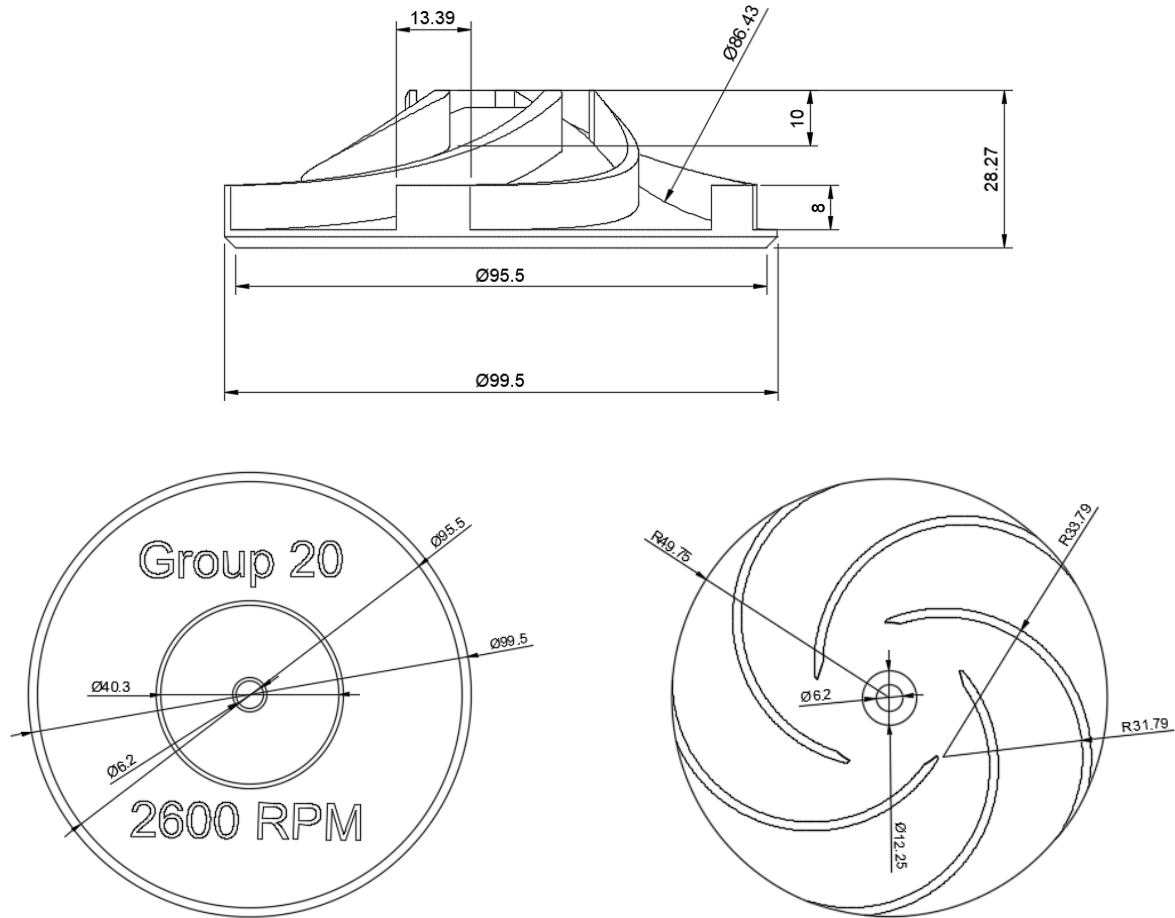


Figure 2.25 & 2.25: Front and top view impeller dimensions

Final Impeller Design Parameters:

Design Paramters	Value
Number of Blades	5
Inner Radius (m)	0.017
Outer Radius (m)	0.05
Inlet Blade Height (m)	0.01
Outlet Blade Height (m)	0.008
Inlet Blade Thickness (m)	0.002
Outlet Blade Thickness (m)	0.002
Inlet Blockage Factor	0.75
Outlet Blockage Factor	0.76
Outlet Blockage Factor Mismatch	0.000005
Inlet Blockage Factor Mismatch	0.000016
Leading Edge Angle (degrees)	22.02
Trailing Edge Angle (degrees)	8.14
Velocity Mismatch (m/s)	1.83
Outflow Angle Disalign (degrees)	0.78
Speed (rpm)	2600
Net Head (m)	11.42

Figure 2.26: Chosen impeller design parameters.

3 Material Analysis and Selection

3.1 Preliminary Calculations

The minimum pressure and maximum deflection the impeller blades should withstand will be calculated:

Minimum pressure:

The VAD will be placed in the left ventricle whereby the average peak systolic and diastolic pressures are 130 and 10 mmHg respectively [2]. The systolic pressure will be used. A safety factor of 2.5 is the norm for medical devices.[3]. The pressure rise of 0.80 bar will also be added on:

$$P_{systolic} = 130 \text{ mmHg} = 130 \times 13.133.22 = 17332 \text{ Pa}$$

$$P_{total} = P_{systolic} + \Delta P = 17332 \text{ Pa} + 80000 \text{ Pa} = 97332 \text{ Pa}$$

$$\therefore P = 97332 \text{ Pa} \times 2.5 = 243.33 \text{ kPa}$$

The **yield strength** has the same units as **pressure** therefore the **minimum yield strength** should far exceed this value.

Maximum deflection:

With the impeller blade modelled as a plate here, it can be said that the deflection should not exceed half the thickness. The chosen impeller's blade thickness is 2mm:

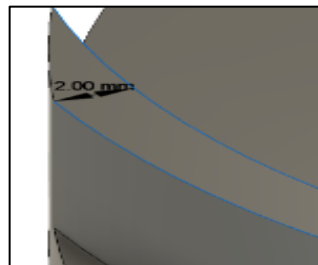


Figure 3.1: Impeller blade thickness

$$\therefore \delta_{max} \leq \frac{0.002m}{2} = 0.001m$$

3.2 Relevant Material Constraints

Material Property	Constraint	Justification
Stiffness	Deflection should not exceed 0.001m calculated.	It is imperative that the impeller blades are rigid to resist deformation which could lead to cavitation and uneven blood flow.
Strength	Should have a minimum yield strength of 243.33kPa as calculated.	High pressure from blood flow could plastically deform the impeller blades. It is vital to ensure the blade's yield strength is beyond the systolic pressure.

Corrosion Resistance & Waterproof	Should be both corrosion resistant and waterproof. Should abide by IEC 60529 standards such as the IP67 or IP66 ratings. This indicates protection against powerful water-jets.	Although the impeller is housed within a casing, it is vital it is waterproof since it is still situated within the human body. Frequent contact with bodily fluids means it is imperative the blades are corrosion resistant.
Biocompatible	Should abide by ISO 14708 standards [5]. Should be approved by the FDA (Food and Drug Administration).	The impeller and casing will be placed within the body. Therefore, if it were not biocompatible it could trigger responses from the immune system as well as tissue irritation which could lead to health complications.
Economic Viability (Cost)	Cost should be minimised however account for average LVAD prices of £80,000 [4].	VADInc does have limited funds where economic viability is a key metric for success of the impeller. However, the profit margins possible with LVAD's are huge and should be considered.

Table 3.2: FOCs and free variables used in material selection.

3.3 Translation of Required FOCs and Derivation of Material Performance Indexes (MPIs)

The constraints and objectives taken forward to the material selection process along and associated free variables are as follows:

Function	Objectives	Constraints	Free Variables
Ensure blood is pumped at a sufficient flow rate and pressure.	Minimise mass. Minimise cost.	High Strength High Stiffness	Blade thickness Material Selection

Table 3.2: FOCs and free variables used in material selection.

To first begin the process of deriving the MPIs, it is essential to first ensure a suitable shape is used to model the impeller blades. For simplicity, the individual impeller blade would be assumed to be a cantilevered plate with a distributed load across its top face:

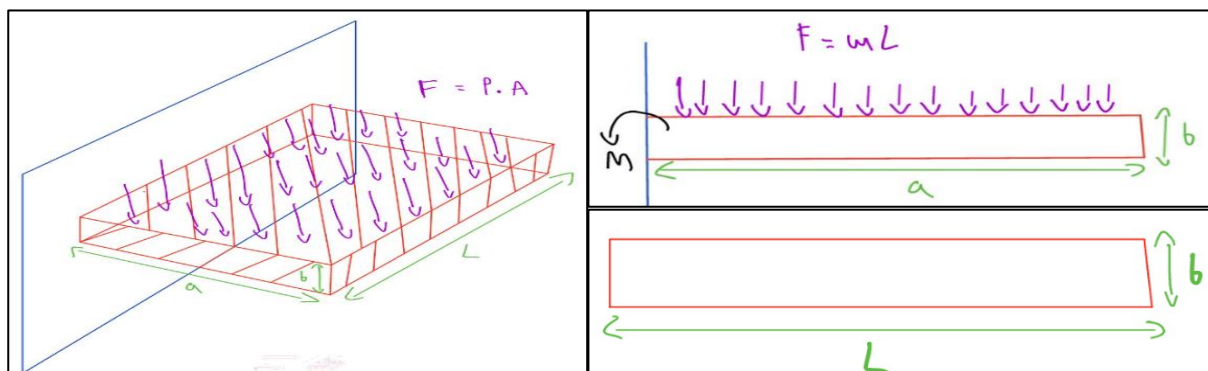


Figure 3.2, 3.3 and 3.4: Schematics showing an impeller blade tilted sideways receiving impact from blood flow.

$$a = \text{blade height} \quad L = \text{blade length} \quad b = \text{blade thickness}$$

Material Performance Indexes Derivation:

Both the MPIs for maximising strength and minimising cost (MPI_1) as well as maximizing strength and minimising mass (MPI_2) will be considered here:

Objective equations:

$$m = pAL \rightarrow m = pabL \quad (3.1)$$

$$C = C_m m \rightarrow C = C_m pabL \quad (3.2)$$

Constraint equation:

$$S = \frac{F}{\delta} \quad (3.3)$$

$$\delta = \frac{Fa^3}{C_1 EI} < \delta_{max}; \text{ where } C_1 = 8 \quad (3.4)$$

The maximum deflection equation is due to the assumption that the impeller blade can be modelled as a beam with a distributed load across its length.

$$I = \frac{Lb^3}{12} \quad (3.5)$$

This is the case here as the beam is of a rectangular cross-section as an assumption of the impeller blade shape as shown in [figure 3.3.1](#). This can be substituted into (3.3) to rearrange for the free variable, b :

$$\delta = \frac{Fa^3}{C_1 E \left(\frac{Lb^3}{12} \right)} \rightarrow b = \sqrt[3]{\frac{12Fa^3}{\delta C_1 EL}} \rightarrow b = a \sqrt[3]{\frac{12F}{\delta C_1 EL}} \quad (3.6)$$

The free variable can now be substituted into the objective equation:

$$m = pabL \rightarrow pLa^2 \sqrt[3]{\frac{12F}{\delta C_1 EL}} \quad (3.7)$$

Separating out into the relevant [material properties](#), [geometric](#) and [functional](#) constraints result in the following equation:

$$m = \left(\frac{p}{E_y^{\frac{1}{3}}} \right) \times La^2 \times \left(\sqrt[3]{\frac{12F}{\delta C_1 L}} \right) \quad (3.8)$$

The objective is to minimise cost so the material property equation in blue would be minimised. It is more convenient to have a maximising equation. The inverse of the equation would need to be maximised leading to our first MPI shown below:

$$\text{Minimise } \left(\frac{p}{E_y^{\frac{1}{3}}} \right), \therefore \text{maximise } \left(\frac{E_y^{\frac{1}{3}}}{p} \right) \quad (3.9)$$

$$\therefore MPI_1 = \left(\frac{E_y^{\frac{1}{3}}}{p} \right) \quad (3.10)$$

Equation (3.8) can be used for the cost-based objective equation (3.2):

$$C = C_m m \rightarrow C = \left(\frac{C_m p}{E_y^{\frac{1}{3}}} \right) \times La^2 \times \left(\sqrt[3]{\frac{12F}{\delta C_1 L}} \right) \quad (3.11)$$

The material property is shown in blue and must be minimised to minimise cost. The inverse is taken for convenience which has to be maximised and will be the MPI:

$$\text{Minimise } \left(\frac{C_m p}{E_y^{\frac{1}{3}}} \right), \therefore \text{maximise } \left(\frac{E_y^{\frac{1}{3}}}{C_m p} \right) \quad (3.12)$$

$$\therefore MPI_2 = \left(\frac{E_y^{\frac{1}{3}}}{C_m p} \right) \quad (3.13)$$

Both the MPIs for maximising stiffness and minimising cost (MPI_3) as well as maximizing stiffness and minimising mass (MPI_4) will be considered here:

The strength-based constraint and mass-objective equations will be defined below:

Objective equations:

$$m = pAL \rightarrow m = pabL \quad (3.14)$$

$$C = C_m m \rightarrow C = C_m pabL \quad (3.15)$$

Constraint equation:

$$F = cZ \frac{\sigma_y}{a} \rightarrow Z = \frac{Lb^2}{6} \text{ and } c = 2 \quad (3.16)$$

The derivation will initiate by first re-arranging equation (3.2) to ensure the variable b is made the subject. This is the free variable whereby the constraint equation will be a function of. This is shown below as follows:

$$b^2 = \frac{6Fa}{Lc\sigma_y} \rightarrow b = \sqrt{\frac{6Fa}{Lc\sigma_y}} \quad (3.17)$$

The free variable can now be substituted back into the objective equation (3.1):

$$m = pabL \rightarrow m = pa \sqrt{\frac{6FL}{Lc\sigma_y}} L \quad (3.18)$$

The equation will now be separated out into the functional constraints, geometric constraints and material properties:

$$m = \left(\frac{p}{\sigma_y^{\frac{1}{2}}} \right) \times aL \times \left(\sqrt{\frac{6FL}{Lc}} \right) \quad (3.19)$$

Therefore, the MPI is as follows:

$$\text{Minimise } \left(\frac{p}{\sigma_y^2} \right), \therefore \text{maximise } \left(\frac{\sigma_y^2}{p} \right) \quad (3.21)$$

$$\therefore MPI_3 = \left(\frac{\sigma_y^2}{p} \right) \quad (3.22)$$

Equation (3.19) can be used for the cost-based objective equation (3.15):

$$C = C_m m \rightarrow C = \left(\frac{C_m p}{\sigma_y^2} \right) \times \alpha L \times \left(\sqrt{\frac{6FL}{Lc}} \right) \quad (3.23)$$

The equation relating the material properties shown in blue must be minimised to meet the mass objective therefore the inverse will be maximised which would be the MPI used for analysis:

$$\text{Minimise } \left(\frac{C_m p}{\sigma_y^2} \right), \therefore \text{maximise } \left(\frac{\sigma_y^2}{C_m p} \right) \quad (3.24)$$

$$\therefore MPI_4 = \left(\frac{\sigma_y^2}{C_m p} \right) \quad (3.25)$$

3.4 Material Selection Process

Screening Process:

It is first useful to eradicate any material groups that will be unsuitable for the impeller of the VAD. The limits for this process included as follows:

- Water resistant.
- Oxygen gas resistant (together with water ensures corrosion resistance).
- 10GPa minimum Young's Modulus. Polyurethane LVADs have a yield strength of 6.84MPa. Since our predominant group are metal alloys, this would be made much higher [22].
- A minimum 10 GPa Yield Strength value.

The Ashby plot pre and post screening are as follows:

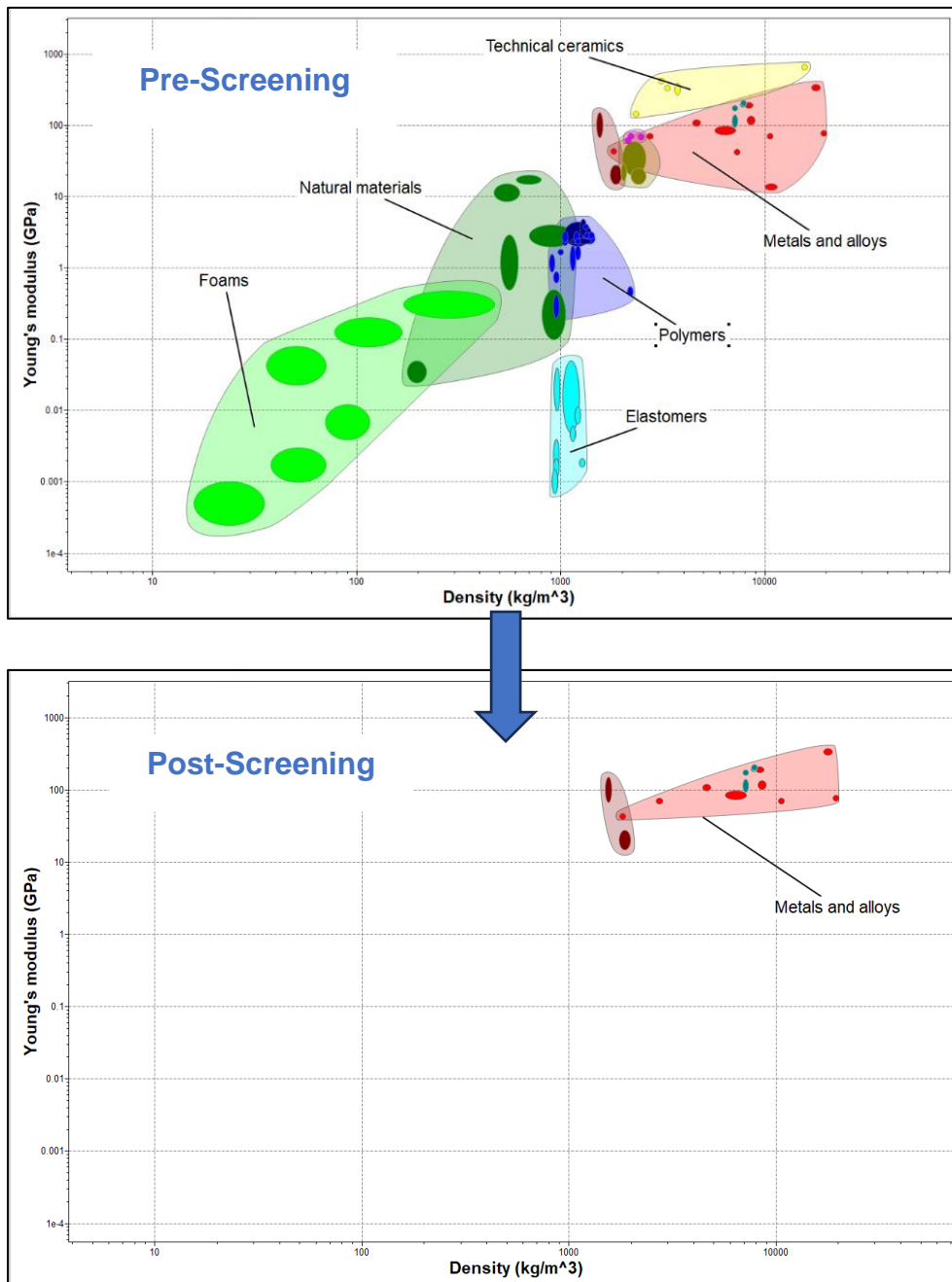


Figure 3.3 and 3.4: Ashby plot pre and post the screening process.

After conducting the screening process, metals and alloys are deemed the most suitable material types for the impeller of the VAD which is expected as are generally used for medical devices. Further filtering is required to limit the materials choices further.

Ranking Process:

The MPIs derived previously will be plotted to further narrow down the selection process. Since these are plotted on a logarithmic scale, a breakdown of the line equation and slope derivation is shown below:

$$MPI_{example} = \frac{y^n}{x} \quad (3.26)$$

$$\rightarrow \log (MPI_{example}) = \log(y^n) - \log(x)$$

$$\rightarrow n\log(y) = \log(x) + \log (MPI_{example})$$

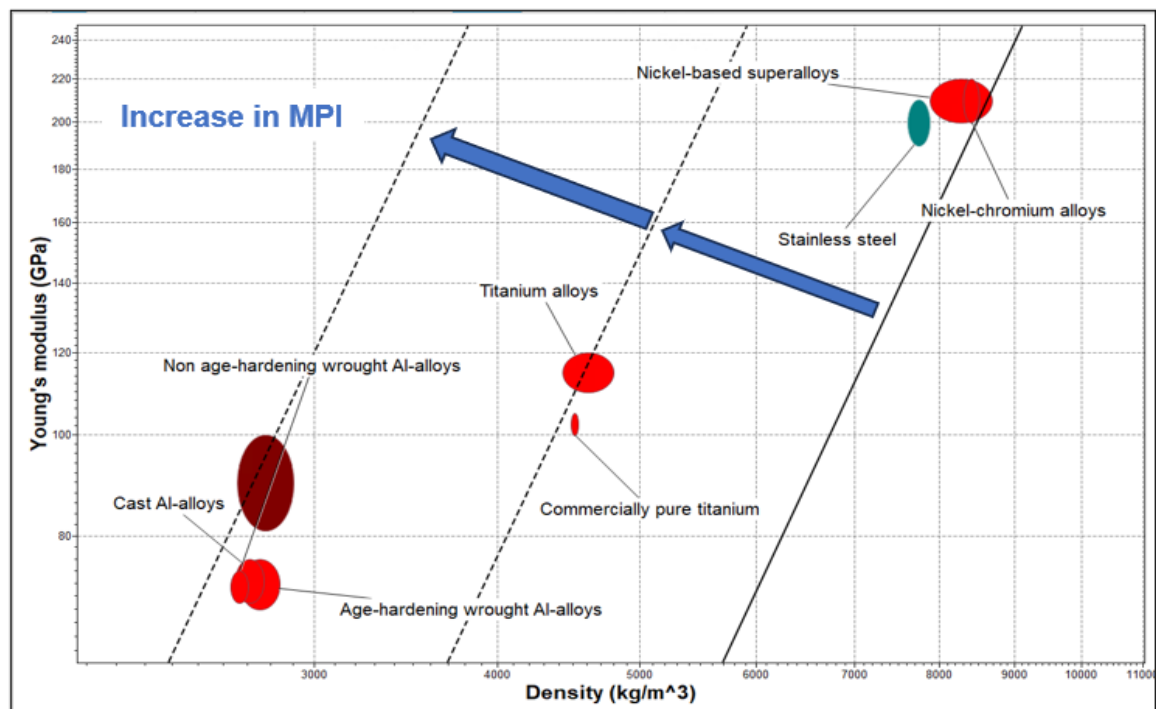
$$\therefore \log(y) = \frac{1}{n}\log(x) + \frac{1}{n}\log (MPI_{example})$$

The slope of this MPI equation would be $\frac{1}{n}$ whilst the y intercept would be $\frac{1}{n}\log (MPI_{example})$.
A table showing the logarithm equations for the 4 MPIs derived previously is shown below:

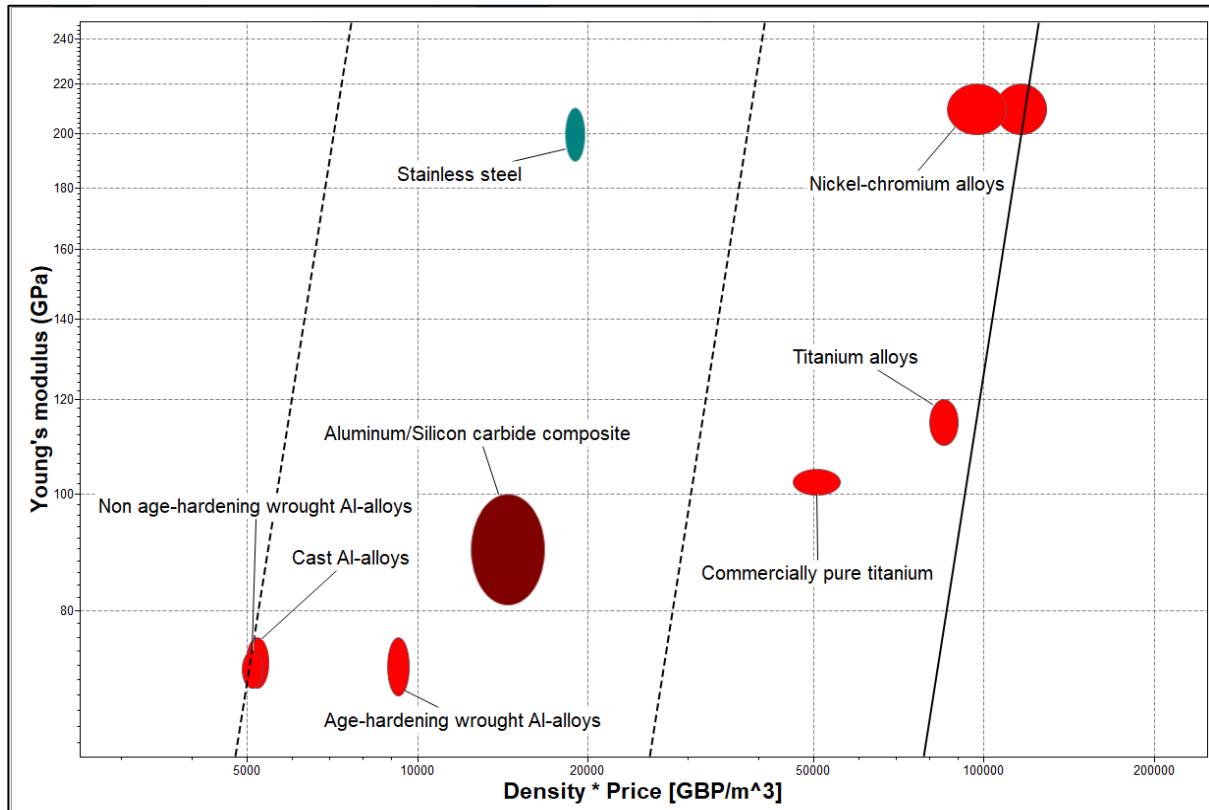
MPI	Logarithmic Equation	Slope
$MPI_1 = \frac{E^{\frac{1}{3}}}{\rho}$	$\log(E) = 3\log(\rho) + 3\log (MPI_1)$	Slope = 3
$MPI_2 = \frac{E^{\frac{1}{3}}}{C_m\rho}$	$\log(E) = 3\log(C_m\rho) + 3\log (MPI_2)$	Slope = 3
$MPI_3 = \frac{\sigma_y^{\frac{1}{2}}}{\rho}$	$\log(\sigma_y) = 2\log(\rho) + 2\log (MPI_3)$	Slope = 2
$MPI_4 = \frac{\sigma_y^{\frac{1}{2}}}{C_m\rho}$	$\log(\sigma_y) = 2\log(C_m\rho) + 2\log (MPI_3)$	Slope = 2

The graphs for each MPI are shown below:

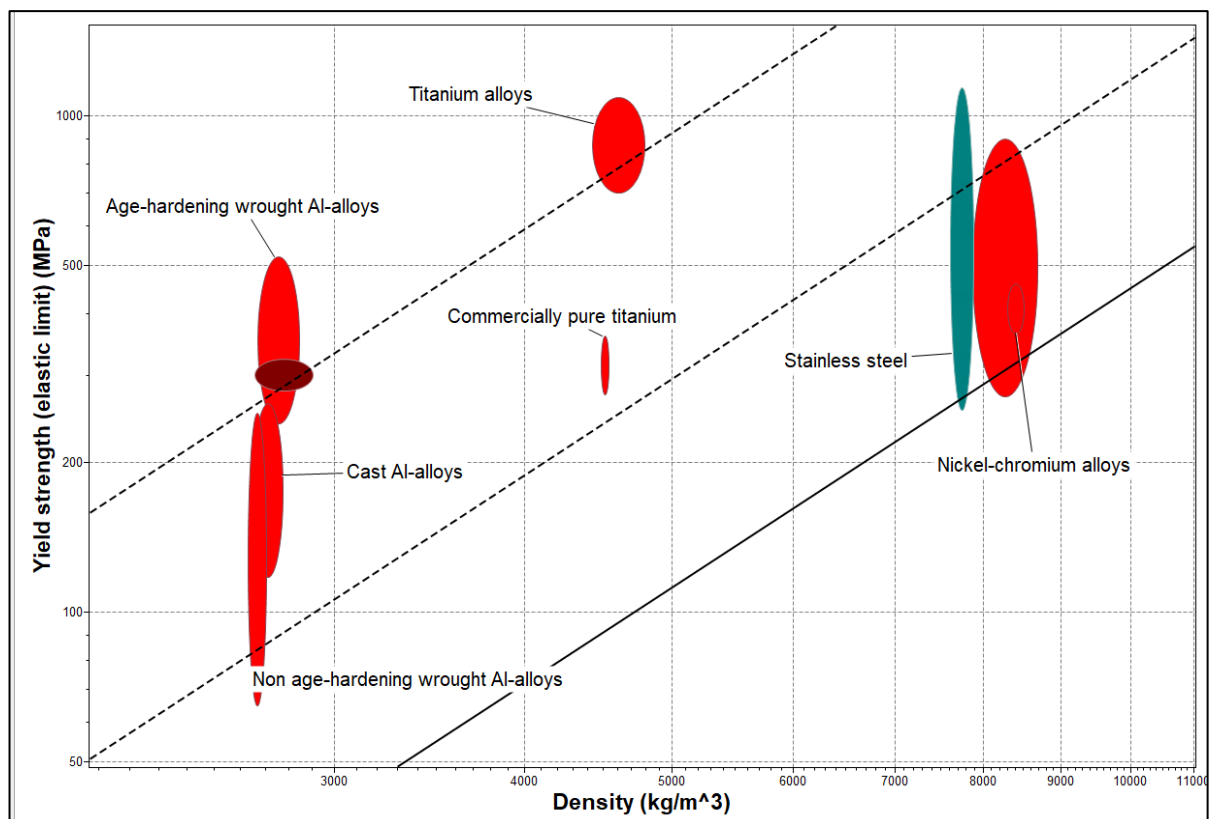
$$MPI_1: \frac{E^{\frac{1}{3}}}{\rho}$$



$$MPI_2: \frac{E^{\frac{1}{3}}}{C_m \rho}$$



$$MPI_3: \frac{\sigma_y^{\frac{1}{2}}}{\rho}$$



$$MPI_4: \frac{\sigma_y^{\frac{1}{2}}}{C_m \rho}$$

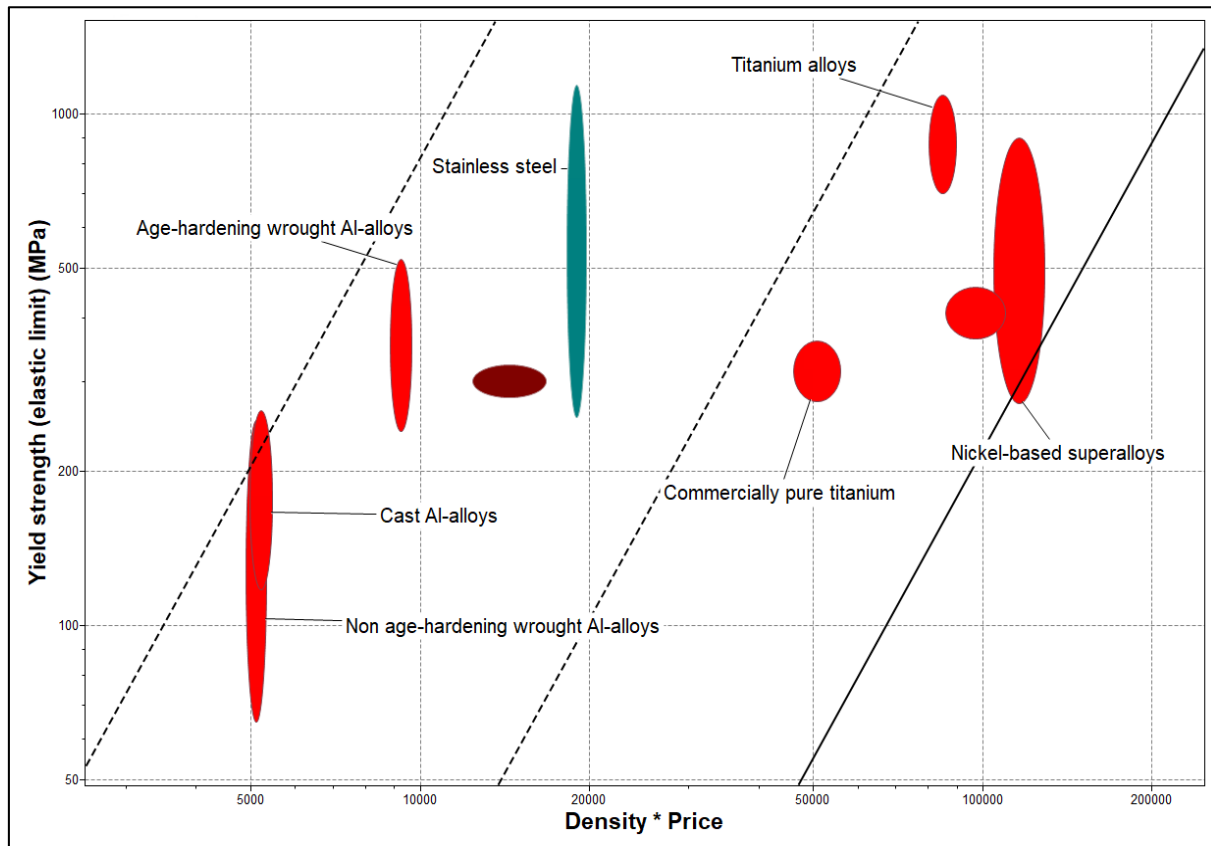


Figure 3.5, 3.6, 3.7 & 3.8: Ashby plots of the 4 MPIs.

Having filtered out the Ashby plots through increasing the MPI gradually as well as the screening process, metal alloy are the predominant choices however more specifically the aluminium, titanium and nickel alloys. Stainless steel can also be seen to be a viable option based on these plots. A table comparing their properties and uses can be seen below:

Material	Uses and Properties
Titanium Alloys	Consists of a high strenght-to-weight ratio, around 25% greater than the best alloys of aluminium or steel. Can be used up to temperatures of 500 degress celcius. Used in for jet engine blades.
Stainless Steel	Most stainless steels resist corrosion in most normal environemtns. Used in a vairyety of applications including toasters and scissors.
Aluminium Alloys	Good machinability whereby it can be formed by both casting and deformation. Used extensively throughtout aerospace industry. It is also relatively light and cheap.
Nickel Alloys	Consists of a high melting point of 1450 degrees. It is used in forming the heatig elements of electric fires and toasters. Nickel superalloys have high temperature strength and good corrosion resistance.

Figure 3.9: 4 main material types along with description.

The material selection still must be narrowed down further. The objectives of mass and cost are conflicting in that some material groups such as the Titanium group perform well when the MPI aims to minimise mass but have high strength but is affected majorly when the cost is involved in which it is one of the lesser viable material choices out of the remaining filtered ones. Stainless steel is an example where the opposite occurs. When assessing against mass alone, it doesn't perform as well being on the heavier end, however when cost is considered becomes a viable option. It is therefore necessary a trade-off between the objectives of minimising mass and cost is considered in making a suitable material decision.

A trade-off curve will be used between the MPIs based around the strength constraint for both objectives of minimising mass and cost. This can be shown below:

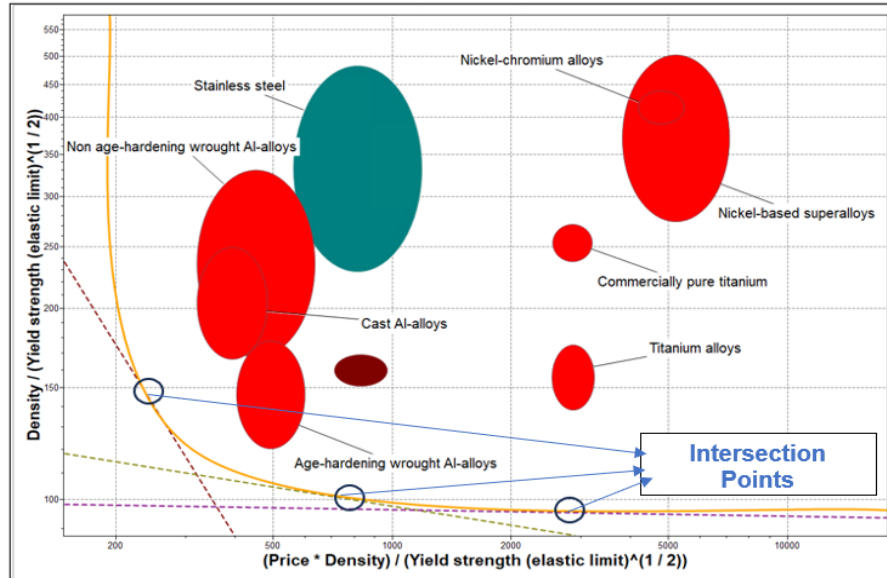


Figure 3.10: Trade-off curve of strength/mass MPI inverse against strength/cost MPI inverse.

The material property equation that would minimise the cost and mass objective equations was used not the inverse to maximise this as seen with the derivation of the MPIs. Penalty function lines were also used here to see the materials that would optimise between both objectives. Derivation of the penalty function can be seen below:

$$M_2 = \frac{\rho}{\sigma_Y^2} \text{ and } M_1 = \frac{C_m \rho}{\sigma_Y^2} \quad (3.27)$$

The penalty function is as follows:

$$Z = \alpha_1 C_1 + \alpha_2 C_2$$

Cost and mass are the objectives so are C_1 and C_2 . Z can be measured in terms of currency due to cost being an objective therefore leaving the exchange constant α_1 as 1.

$$\therefore Z = C + \alpha_2 m \quad (3.28)$$

Since the MPIs used are cost and mass based the following can be said:

$$Z = M_1 + \alpha_2 M_2 \quad (3.29)$$

$$\therefore M_2 = -\frac{1}{\alpha} M_1 + \frac{1}{\alpha} Z \quad (3.30)$$

Since Z is too be minimised, points of intersection between the penalty line and trade of surface are preferred. Figure 3.10 shows 3 different exchange constants varied using 1, 10 and 100 GBP/kg. Lower exchange constants favour aluminium alloys due to being closer to the point of intersection whereas higher exchange constants make titanium alloys more favourable. This means the value of titanium saved is valued higher which is suitable here since although VADInc have limited funds, the impeller would be light therefore not a dear material price. The return of investment of these products are quite high with LVADs averaging at a price of £80000. This can excuse a trade off in cost for mass as this is an implantable device so it is crucial mass is minimised regardless. The added strength titanium does provide. A small batch size for manufacture with an example LVAD known as the Heart Mate 3 weighing 0.3kg [7], titanium alloys do prove to be a strong solution in this context.

Stainless steel and the **Nickel-based alloys** are dominated solutions here being further away from the

The Fatigue Strength at 10^7 cycles will be compared for each material in the trade-off curve since than important property as LVADs is normally used for around 5-6 years for each person [8] and since the heart pump around 100,000 times in a day [6], the impeller must withstand high pressure cyclic loading continuously. The graph can be seen below:

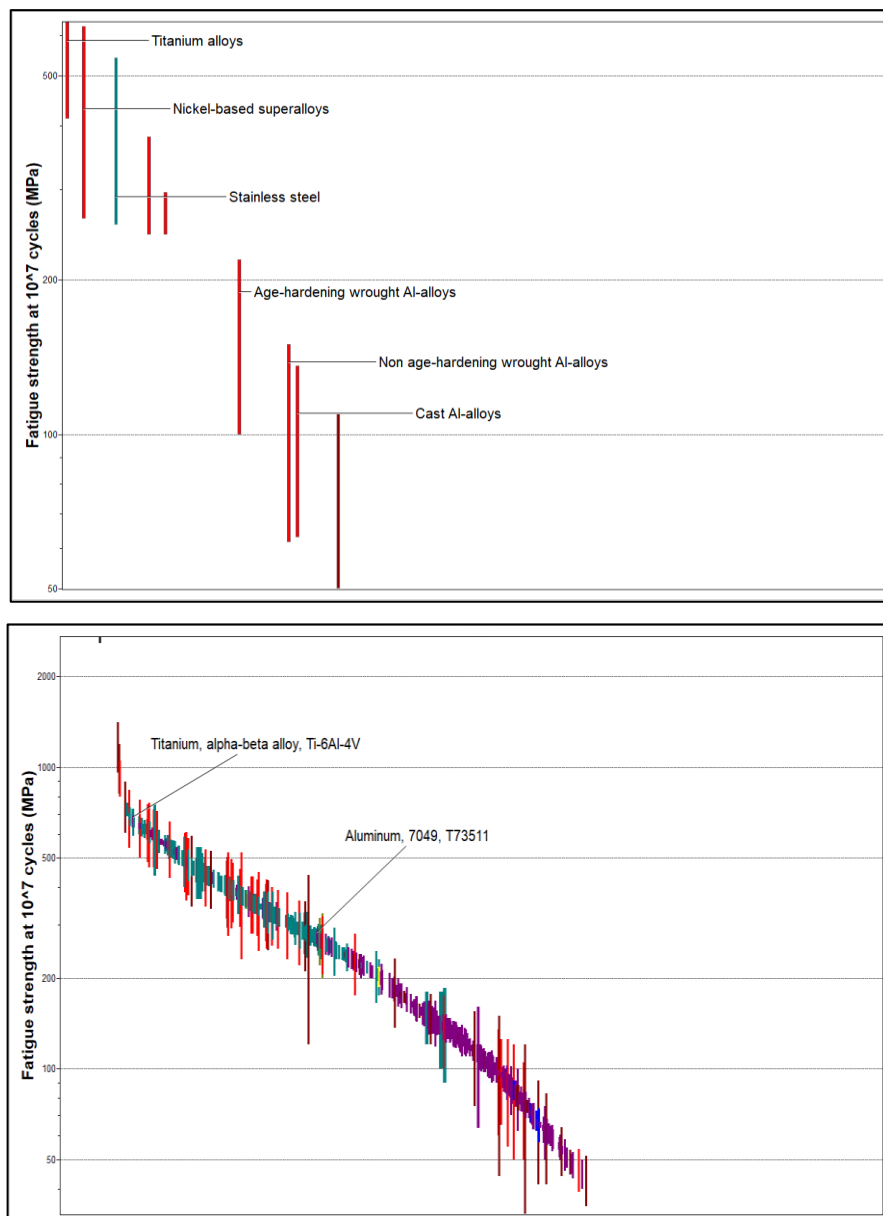


Figure 3.11 and 3.12: Fatigue strength at 10^7 cycles at Levels 2 and 3.

Titanium is the better option than aluminum for this material property as shown from the bar charts, in fact being the best metal alloy group and so a great option in this case. 2 of the best grades for each of the titanium and aluminum groups were used in which further showed Titanium's better strength. Titanium is also biocompatible and used extensively throughout the medical industry.

The results and analysis show titanium alloys are the best material group for this use. The Titanium Ti-6Al-4V grade seems a viable option proven by its high strength and other properties including good corrosion resistance and biocompatibility. The properties are as follows:

Titanium TI-6Al-4V	
Properties	Metric
Young's Modulus	110-119 GPa
Yield Strength	786-910 MPa
Cost	17.6-20.9 GPB/kg
Density	$4.43 \times 10^3 \text{ kg/m}^3$
Fatigue Strength at 10^7 Cycles	327-381 MPa
Fracture Toughness	84-107 MPa.m ^{0.5}
Biocompatible	Yes

5 Manufacturing Method Analysis and Selection

5.1 Translation of Design Requirements and Screening Process

The mass of the model impeller is now known due to the material choice known. The properties of the model impeller are shown below:

Mass	288.722 g
Volume	65174.349 mm ³
Density	0.004 g / mm ³
Area	25507.589 mm ²

Figure 4.1: Impeller CAD model properties from Fusion 360



Figure 4.2: Realistic EVAHEART LVAD pump

The model must be scaled to account for realistic dimensions of a LVAD impeller. The Evaheart centrifugal pump contains an impeller of a diameter of 40mm [8]. It is assumed here that the linear scale factor is the same for all dimensions including impeller height. The linear scale is as follows:

$$\frac{\text{Model impeller outer diameter}}{\text{Evaheart LVAD impeller diameter}} = \frac{99.5\text{mm}}{40\text{mm}} = 2.4875 \quad (4.1)$$

The linear scale factor is 2.4875, therefore the volume scale factor would this value cubed. With a known model mass and the mass and volume being directly proportional due to $m = \rho V$, the realistic mass used is:

$$\frac{\text{Model mass}}{(\text{Linear scale factor})^3} = \frac{288.722g}{(2.4875)^3} = 18.76g \quad (4.2)$$

A table for the process requirements of the scaled impeller can be seen below:

Process Requirements for the Impeller	
Function	Ensure blood is pumped at a sufficient flow rate and pressure around the body.
Constraints	<u>Material</u> : Titanium Ti-6Al-4V Annealed
	<u>Shape</u> : 3D Solid
	<u>Estimated Mass</u> : 0.01 - 0.06kg
	<u>Section Thickness</u> : 4mm
	<u>Tolerance</u> : $\pm 0.5\text{mm}$
	<u>Roughness</u> : $\leq 1.7\mu\text{m}$
	<u>Batch size</u> : 1000 - 1500 units
Objectives	To minimise the cost of production
Free Variables	Choice of Process
	Process-operating conditions

Figure 4.3: Limit values for initial manufacturing process screening.

It should be stated that a primary shaping process is also preferable.

Estimated mass: 0.01 – 0.06kg is a suitable range for the impeller mass with the world's smallest LVAD consisting of an pump weighing 27g [9].

Tolerance: The maximum tolerance used in the impeller design is 0.5mm as seen in Figure 2.23 and so is applied here.

Batch size: VADInc would have a limited batch size due to limited funds. HEARTMATE currently have 1500 implants of their LVAD in Europe [10]. Although their batch size of production would be more, a start-up such as VADInc would prevent excess production as much as possible hence this value has been taken.

Roughness: LVAD impellers normally have surface roughness values below $1\mu\text{m}$ [11] however a range up to $1.7\mu\text{m}$ Was used since manufacturing processes can normally provide better roughness values than the stated amount:

Process notes

Most processes will be able to achieve roughness (or smoothness) levels better than the stated range. However, there will be an associated increase in cost, which may be large.

Using these constraints meant only **7 out of 146** manufacturing methods were left to choose from. A graph of the surface roughness ranges of each manufacturing process pre and post screening is shown below to show this:

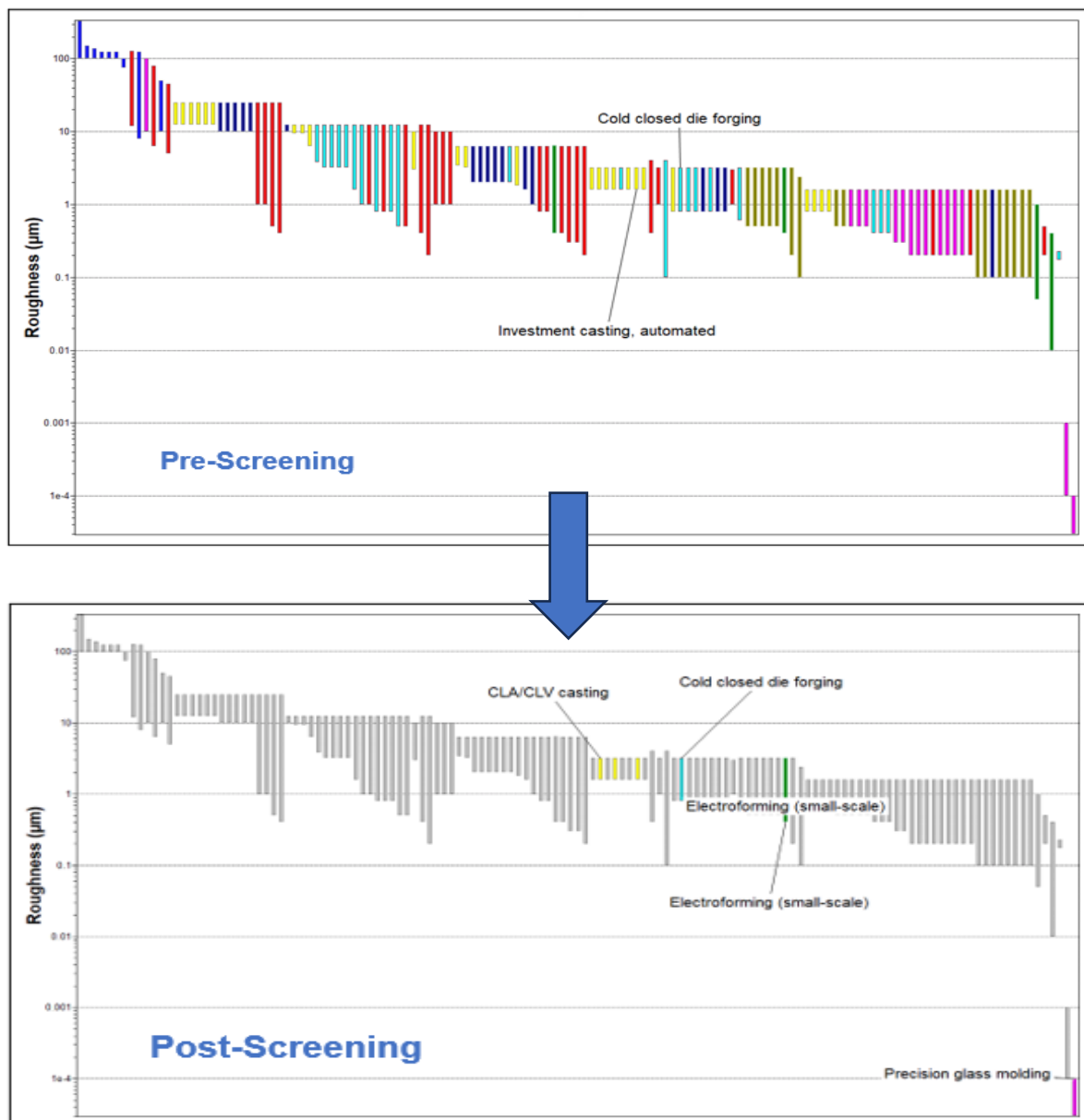


Figure 4.4: Roughness against Materials Pre and Post Screening

The manufacturing methods left over are:







-  CLA/CLV casting
-  Cold closed die forging
-  Electroforming (small-scale)
-  Investment casting
-  Plaster mold casting
-  Precision glass molding

Figure 4.5: Remaining manufacturing processes.

The economic based properties of each of these processes will now be compared:

Manufacturing Process & Metrics	CLA/CLV Casting	Cold Closed Die Forging	Electroforming (small-scale)	Investment Casting (automated)	Plaster Mold Casting	Precision Glass (molding)
Capital Cost (£)	4.141e4 - 1.03e5	2.94e5-7.35e5	1.47e4-7.35e4	1.47e4-7.35e4	1.47e3-7.35e3	3.9e4-7.8e5
Production Rate (units)	1-100	100-500	0.1-1	10-200	0.5-10	2.0-20
Tool Life (units)	500-5e3	1e3-1e6	1-1e3	500-5e3	500-5e3	100-500
Tooling Cost (£)	1.47e3-2.21e4	4.41e3-1.32e4	147-4.41e3	1.47e3-2.21e4	294-1.47e3	1.47e3-1.47e4
Relative Cost Index (£ per unit)	28-154	13.7-27.8	403-1.76e3	15.8-57.2	22.6-245	42.3-145

Figure 4.6: Economic properties of each manufacturing process.

- **Electroforming** will not be one of the processes considered going as it does have the highest relative cost index range which goes against the objective of minimising cost.
- The **precision glass process** has a very low range for tool life compared to the other processes and with one of the highest ranges for **capital cost**, this would result in an expensive process which is not feasible for a start-up such as VADInc therefore **will also not** be considered going forward. It's mainly used to create glass components which is not the case here.
- **Plaster Mold casting** does consist of a **low production rate** which is also seen with the electroforming and precision glass moulding processes. This would mean less impellers are produced in a specific time frame which could make investment less attractive for investors which is a huge disadvantage for a start-up as such. When manufacturing at larger scales, this would be a huge disadvantage requiring a change in the process. The **relative cost index** is also like other process including investment casting which have higher production rates therefore is another process not considered in the final selection process.

The 3 remaining manufacturing processes are therefore **CLA/CVA Casting, Cold Closed Die Forging and Investment Casting (automated)**. A Part Cost vs Batch Size graph is shown below for these 3 processes used to make the impeller:

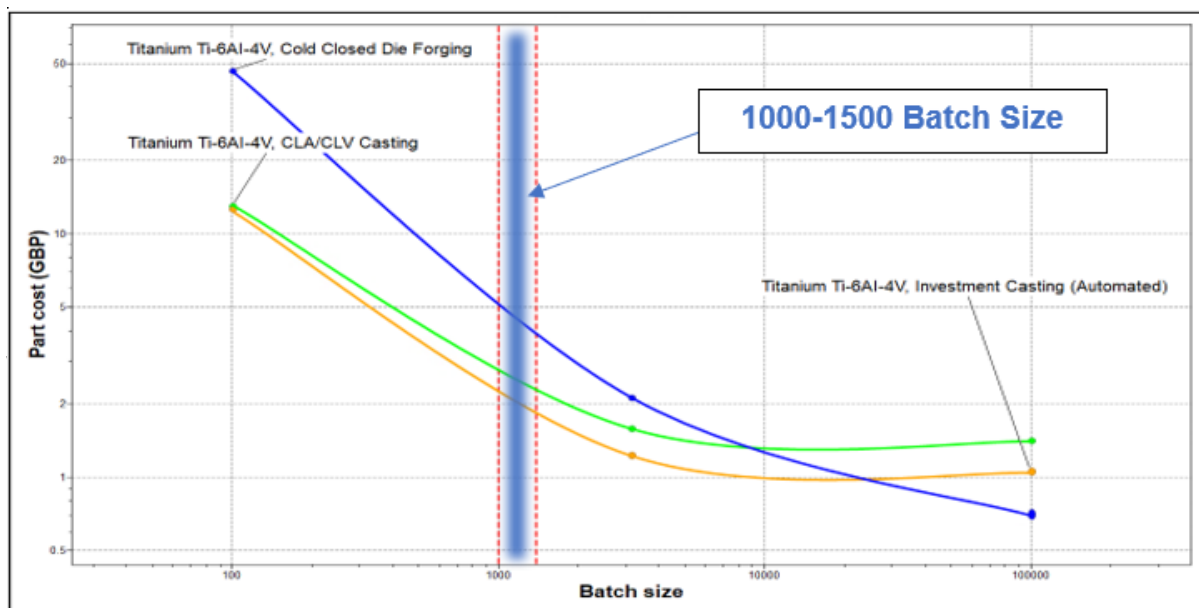


Figure 4.7: Part Cost vs Batch Size for the 3 different processes for Titanium Ti-6Al-4V

process means prices at around £2.10 for this batch size however although this process is used for a range of alloys, it is predominantly used for ferrous alloys whereby titanium is non-ferrous. This means that this process will not be considered for a final manufacturing process choice.

Investment casting and Cold Closed Die Forging are therefore the final 2 process for selection. Graphs for the production rate and relative cost per index against the batch size for both are plotted below:

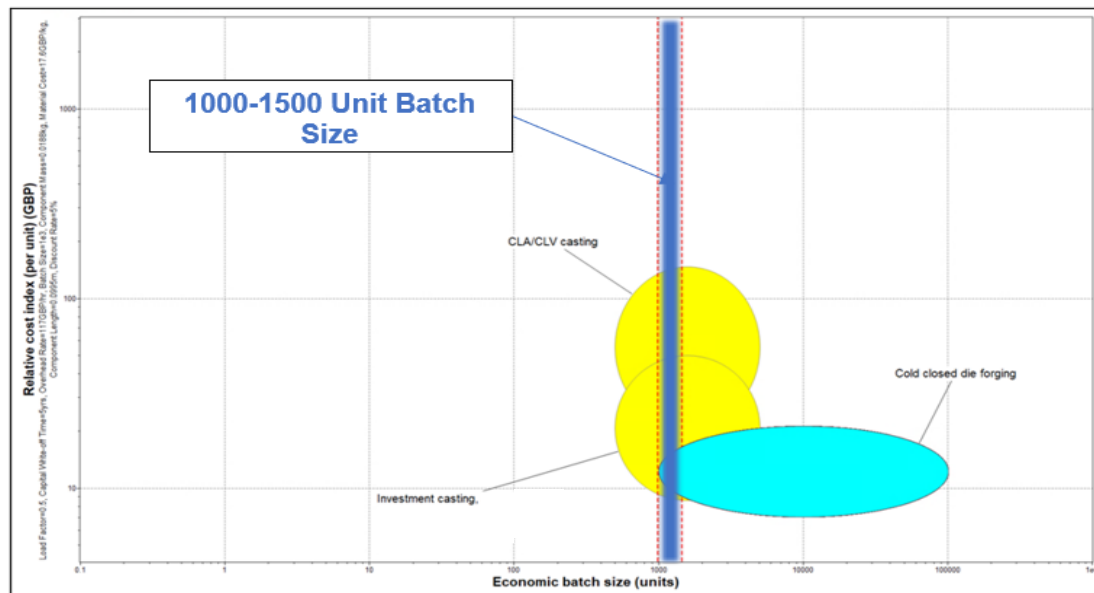


Figure 4.8: Relative Cost Index vs Economic Batch Size

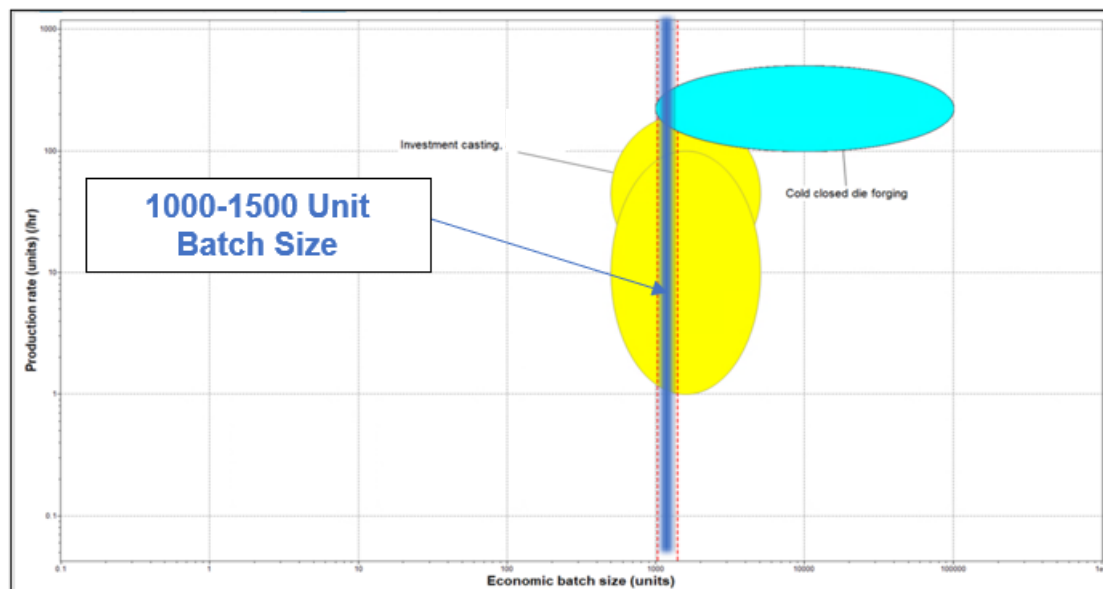


Figure 4.9: Production Rate vs Economic Batch Size

Figure 4.8 shows that for a batch size of 1000-1500 units, investment casting can provide lower values than die forging for the relative cost index, meaning at a value of £8 compared to £9 per unit for cold die forging. This goes in line with the part cost results stated before,

showing that production of the impeller LVAD would be cheaper with the use of investment casting. Figure 4.7 also shows that for a batch size of 1000 for example, it would cost around £4000 if cold closed die forging is used compared to around £2100 with the use of investment casting. Die forging does require forging dies to be made which does require the use tool steel and CNC machining hence the high set-up costs for a complex part [12].

Cold closed die forging does provide higher production rates however as shown in Figure 4.9 for this batch size, a maximum of 300 units per hour compared to 200 units per hour for investment casting. For VADInc, this would not be as much of an issue as cost due to a low batch size and limited funds. Bringing all these points together, as well as **investment casting's** wide use for complex parts, non-ferrous alloys as well as being able to achieve excellent detail replication this would be the **chosen manufacturing process** for the LVAD impeller. A brief insight of the process can be seen below:

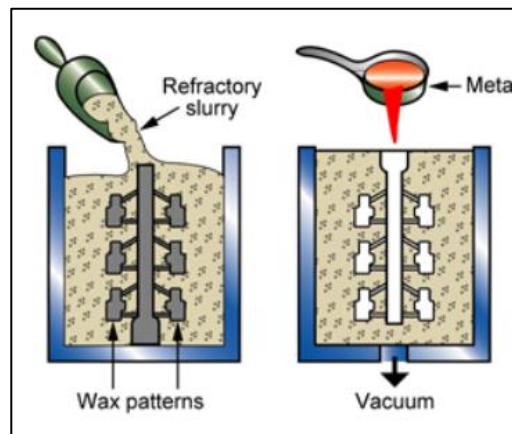


Figure 4.10: Schematic for Investment Casting Process.

- Wax patterns are made by injection moulding into a die then put on a tree with feeding and gating systems.
- These are then inserted into a refractory slurry and covered in a refractory stucco then left to dry.
- This procedure is repeated until around 8 coats of refractory are achieved creating the shell.
- The wax is melted, and the shell heated with the molten metal then poured into the cast.

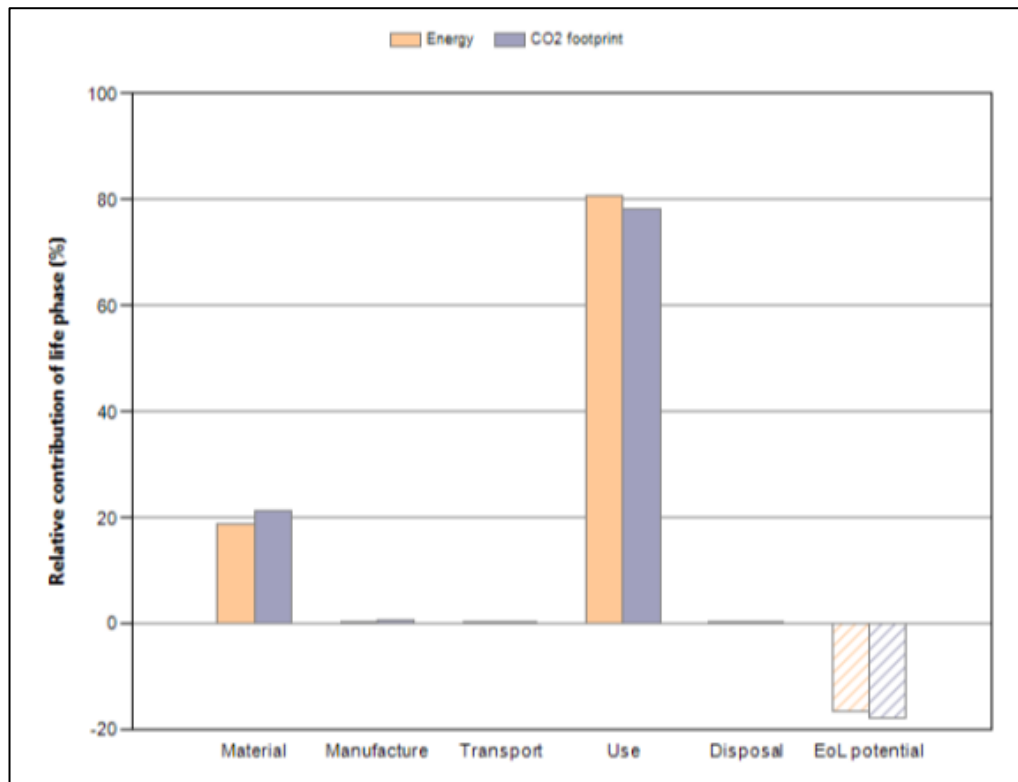
6 Design Sustainability

6.1 Eco-audit Report

The CES Edupack Eco-audit tool is used for sustainability analysis. The variables used are:

Variable Group	Variable Type	Value/Input	Justification
Material, Manufacture and End of Life	Quantity	300	300 people in the UK currently use an LVAD. The quantity distributed would roughly be this amount [15].
	Material	Titanium, Alpha-Beta Alloy, Ti-6Al-4V	The choice of this material has been shown through the material selection process carried out. It is a commonly used material in the medical industry, with properties including good corrosion resistance and a good strength-to-weight ratio.
	Manufacturing Process	Investment Casting	The selection process of this manufacturing process has been shown previously. It is commonly used with non-ferrous alloys which is the case here and is useful for producing complex shapes, suitable for the impeller end product.
	Mass (kg)	0.01875	The scaled down mass is used as this is a realistic impeller value. The world's smallest LVAD weighs 27g and contains driven magnets and an impeller. Therefore the impeller would weigh less than 27g and so 18.75g is feasible [13].
	End of Life Process	Recycle	Titanium's properties means that it is recycled for uses in sectors such as the automotive industry. OrtoMetals is a company that carries out re-melting of titanium from medical devices to ingots to sell [14]. This is done vastly due to titanium's beneficial properties stated before.
Transport	Transport Type	Light Goods Vehicle	Assuming 300 impellers are distributed, the approximate weight onboard is 300 multiplied by 19g which is 5.7kg. Light Goods Vehicles would be sufficient as they tend to carry no more than 3500kg [16].
	Distance (km)	105	To calculate a rough travel distance, the distance between a medical device based in Cambridge known as CMR Surgical and St Bartholomew's Hospital was found as this was one of the first hospital to use LVADs [17].
Use	Product Lifetime (years)	10	The typical amount of years for a person to live with an LVAD is around 5 years [18]. The longest ever ongoing use was around 13 years [19]. 10 years was chosen to be approximately in the midst of this range.
	Country of Use	United Kingdom	VADInc is a start-up with limited funds so unlikely to scale outside of the UK at this stage.
	Energy Input and Output	Mechanical I to Mechanical	A motor drives the impeller, in this case at a speed of 2600rpm. An independent, rechargeable power supply that can be charged whilst implanted is a key focus and will provide this power.
	Power Rating (W)	25	LVADs typically require 5-25W of power and so the maximum will be taken here.
	Usage	365 (days per year)	The LVAD impeller will be operating everyday since blood needs to flow around the body.
		24 (hours per day)	The LVAD impeller will be operating at all times since the heart is constantly beating.

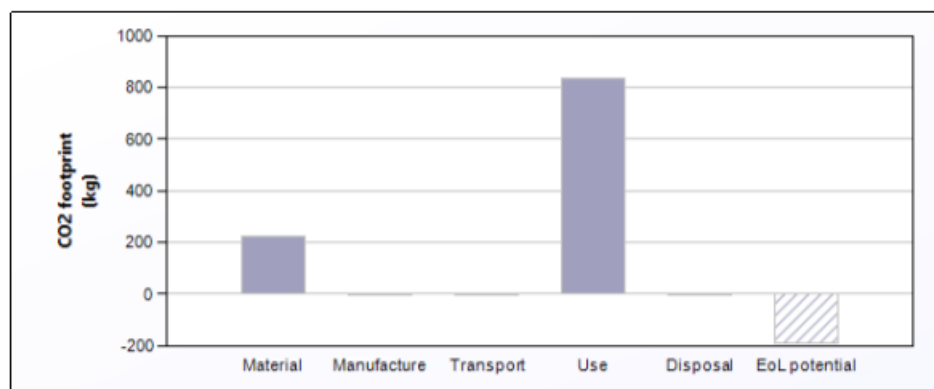
The summary report can be seen below:



Phase	Energy (MJ)	Energy (%)	CO2 footprint (kg)	CO2 footprint (%)
Material	3.87e+03	18.9	227	21.3
Manufacture	74.3	0.4	5.57	0.5
Transport	1.3	0.0	0.0938	0.0
Use	1.65e+04	80.7	833	78.2
Disposal	3.94	0.0	0.276	0.0
Total (for first life)	2.04e+04	100	1.07e+03	100
End of life potential	-3.38e+03		-188	

Figure 4.12: Eco-audit report along with values of each stage of the LCA.

Individual graphs for the energy and carbon footprint at each stage are below:



	CO2 (kg/year)
Equivalent annual environmental burden (averaged over 10 year product life):	107

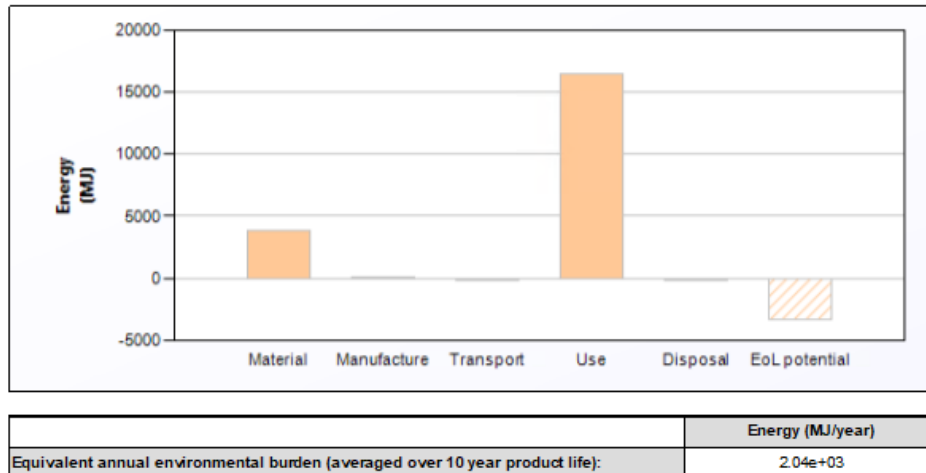


Figure 4.13 and 4.14: Energy and Carbon Footprint for LCA.

6.2 Analysis of Sustainability Results

The summary report here considers 3 parts of the life cycle of the impeller. The first stage would be the extraction and machining of the product, the second stage is the actual usage of the component with the last revolving around the disposal process of the impeller. The usage stage consists of 81% energy consumption and 78% carbon footprint consumption of the whole lifecycle. The power consumed by the impeller is proportional to this with the graphs below representing this with an increment of 5W for the power rating from 5-25W:

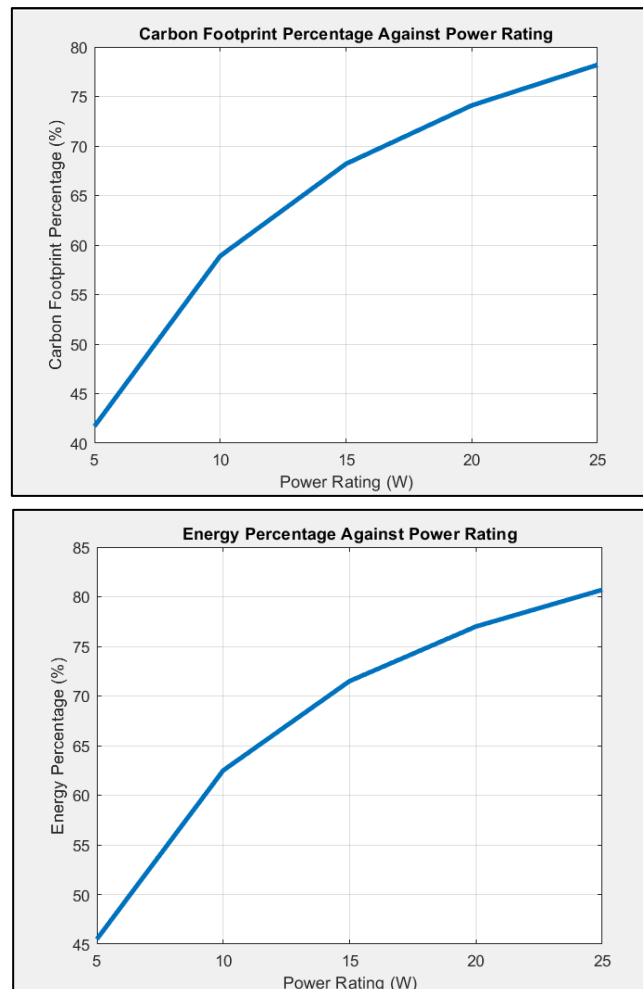


Figure 4.15 and 4.16: Energy and Carbon Footprint Usage Percentage against Power Rating.

The relative energy and carbon footprint consumed in the use stage increase with the power rating of the LVAD pump. The impeller can be redesigned to achieve similar flow rates with a decrease in pressure needed:

Magnetic Levitating Bearings – The DuraHeart LVAD uses these where they eliminate mechanical contacts within the blood chamber. This reduces friction heavily reducing the power needed. Haemolysis and thrombosis are reduced [21].

Closed Impeller Design – These require lower Net Positive Suction Heads meaning it can operate at lower pressure margins. Leakages are minimized, aiding the operational efficiency.

These design changes should be targeted since they could mean lower energy consumed overall. The materials extraction and machining processes also has high relative energy consumption however is the best choice for this scenario and so limited with the changes that can be made. The 'End of Life Potential' being negative does mean the life cycle of the impeller can produce negative effects to the environment mainly due to the extreme temperatures needed to remelt and refine the material. However, this can be hard to mitigate, therefore design changes should be prioritised.

8 Appendix

8.1 References

- [1]: Best Cancer Treatment in India - Join the Fight Against Cancer [Internet]. Cancer Rounds. [cited 2024 Jan 26]. Available from: <https://www.cancerrounds.com/costs/lvad/>
- [1.1]: Robert, Stahovich M, Chillcott S, Baradarian S, Chammas J, Jaski BE, et al. Clinical Strategies and Outcomes in Advanced Heart Failure Patients Older Than 70 Years of Age Receiving the HeartMate II Left Ventricular Assist Device. Journal of the American College of Cardiology. 2011 Jun 21;57(25):2487–95.
- [2]: 7 Tips for Submissions to IEC60601 Edition 3 [Internet]. StarFish Medical. 2013. Available from: <https://starfishmedical.com/blog/7-tips-for-efficient-medical-device-submissions-to-iec-60601-edition-3/>
- [3]: Donnelly B. The Cardiac Cycle - Pressures in The Heart - TeachMePhysiology [Internet]. TeachMePhysiology. 2016. Available from: <https://teachmephysiology.com/cardiovascular-system/cardiac-cycle-2/cardiac-cycle/>
- [4]: From heart failure to health: Pump shown to restore organ to fitness [Internet]. Press Office. [cited 2024 Jan 21]. Available from: <https://www.ncl.ac.uk/press/articles/archive/2017/04/heartpumprestoreshealth/>
- [5]: Iso.org. 2021. Available from: <https://www.iso.org/obp/ui/#iso:std:iso:14708:-1:ed-2:v1:en>
- [6]: 1.How Many Times Does Your Heart Beat in a Day? | Fun Fact Friday [Internet]. Soma Tech Intl's Blog. 2020. Available from: <https://www.somatechnology.com/blog/fun-fact-friday/how-many-times-does-your-heart-beat-in-a-day/>
- [7]: Castagna F, Stöhr EJ, Pinsino A, Cockcroft JR, Willey J, Reshad Garan A, et al. The Unique Blood Pressures and Pulsatility of LVAD Patients: Current Challenges and Future Opportunities. Current Hypertension Reports [Internet]. 2017;19(10). Available from: <https://www.ncbi.nlm.nih.gov/pmc/articles/PMC5645430/>

[8]: Antony M, Tom M, Varghese J, Joseph S, Polachan S. Design, analysis and validation of left ventricular assist device. Materials Today: Proceedings. 2021 Jun;

[9]: Qian KX, Wang DF, Topaz S, Ru WM, Zeng P, Yuan HY, et al. World-smallest LVAD with 27 g weight, 21 mm OD and 5 l min⁻¹ flow with 50 mmHg pressure increase. Journal of Medical Engineering & Technology [Internet]. 2007 [cited 2024 Jan 24];31(3):181–4. Available from: <https://pubmed.ncbi.nlm.nih.gov/17454406/>

[10]: Garbade J, Bittner HB, Barten MJ, Mohr FW. Current Trends in Implantable Left Ventricular Assist Devices. Cardiology Research and Practice. 2011;2011:1–9.

[11]: Takami Y, Makinouchi K, Nakazawa T, Glueck J, Benkowski R, Nose Y. Effect of Surface Roughness on Hemolysis in a Pivot Bearing Supported Gyro Centrifugal Pump (C1E3). Artificial Organs. 2008 Nov 12;20(11):1155–61.

[12]: what are foring dies made out of - Google Search [Internet]. www.google.com. [cited 2024 Jan 25]. Available from: https://www.google.com/search?q=what+are+foring+dies+made+out+of&og=what+are+foring+dies+made+out+of&gs_lcrp=EgZjaHJvbWUyBggAEEUYOTIICAQABgWGB4yDQgCEAAyHgMYgAQYigUyDQgDEAAyHgMYgAQYigXSAQgzNTg4aiBqOagCALACAA&sourceid=chrome&ie=UTF-84The worl

[13]: Qian KX, Wang DF, Topaz S, Ru WM, Zeng P, Yuan HY, et al. World-smallest LVAD with 27 g weight, 21 mm OD and 5 l min⁻¹ flow with 50 mmHg pressure increase. Journal of Medical Engineering & Technology [Internet]. 2007;31(3):181–4. Available from: <https://pubmed.ncbi.nlm.nih.gov/17454406/>

[14]: Cremation and metal implants [Internet]. www.orbitas.co.uk. Available from: <http://www.orbitas.co.uk/news-blogs/blogs/cremation-metal-implants.aspx>

[15]: New tool could lead to improved care of patients living with artificial heart pump [Internet]. University of Birmingham. [cited 2024 Jan 26]. Available from: <https://www.birmingham.ac.uk/news-archive/2019/new-tool-could-lead-to-improved-care-of-patients-living-with-artificial-heart-pump>.

[16]: B.V BMS. What is a light goods vehicle (LGV)? [Internet]. Webfleet. [cited 2024 Jan 26]. Available from: [https://www.webfleet.com/en_gb/webfleet/fleet-management/glossary/light-goods-vehicle/#:~:text=Light%20goods%20vehicles%20\(under%20%2C500](https://www.webfleet.com/en_gb/webfleet/fleet-management/glossary/light-goods-vehicle/#:~:text=Light%20goods%20vehicles%20(under%20%2C500)

[17]: Spotlight on... the LVAD programme at St Bartholomew's Hospital | Our news - Barts Health NHS Trust [Internet]. www.bartshealth.nhs.uk. [cited 2024 Jan 26]. Available from: <https://www.bartshealth.nhs.uk/news/spotlight-on-the-lvad-programme-at-st-bartholomews-hospital-7329#:~:text=Known%20as%20destination%20therapy%2C%20it>

[18]: How Long Can You Live With a Left Ventricular Assist Device? [Internet]. MedicineNet. Available from: https://www.medicinenet.com/survival_rate_with_a_ventricular_assist_device/article.htm#:~:text=A%20patient%20may%20stay%20alive

[19]: Potapov EV, Kaufmann F, Müller M, Mulzer J, Falk V. Longest Ongoing Support (13 Years) with Magnetically Levitated Left Ventricular Assist Device. ASAIO Journal [Internet]. 2020 [cited 2022 Jan 20];66(9):e121. Available from: https://journals.lww.com/asaiojournal/Fulltext/2020/09000/Longest_Ongoing_Support_13_Years_with.19.aspx

[20]: Waters BH, Park J, Bouwmeester JC, Valdovinos J, Geirsson A, Sample AP, et al. Electrical power to run ventricular assist devices using the Free-range Resonant Electrical Energy Delivery system. The Journal of Heart and Lung Transplantation. 2018 Dec;37(12):1467–74.

[21]: Morshuis M, El-Banayosy A, Arusoglu L, Koerfer R, Hetzer R, Wieselthaler G, et al. European experience of DuraHeart™ magnetically levitated centrifugal left ventricular assist system. European Journal of Cardio-Thoracic Surgery [Internet]. 2009 Jun 1;35(6):1020–8. Available from: <https://academic.oup.com/ejcts/article/35/6/1020/473475>

[22]: Left Ventricular Assist Device - an overview | ScienceDirect Topics [Internet]. www.sciencedirect.com. Available from: <https://www.sciencedirect.com/topics/materials-science/left-ventricular-assist-device>

8.2 MATLAB Code

Blade Number Variance vs Key parameters

```
t = 0.002;  
b_1 = 0.011;  
b_2 = 0.006;  
r_2 = 0.05;  
r_1 = 0.017;  
Area = 0.000278;  
Q = 1.5*10^(-3);  
speed = 240.855436775;
```

```
figure()
```

```
outflow_list = [];  
velocity_list = [];  
inlet_blockagefactor = [];  
outlet_blockagefactor = [];
```

```
for n = 5:1:10;
```

```
    for Bf_1 = 0:0.001:1;
```

```
        beta_1 = atand(Q/(2*pi*b_1*Bf_1*speed*((r_1).^2)))*(pi/180);
```

```
        inlet_blockage = 1 - ((n * t * b_1) / (2 * pi * r_1 * b_1 * sin(beta_1)));
```

```
        if abs(Bf_1 - inlet_blockage) < 1e-3;
```

```
            Bf_1;
```

```
            inlet_blockage;
```

```

        inlet_blockagefactor(n-4) = inlet_blockage;

    end

end

for Bf_2 = 0:0.001:1;
    v_2n = (Q./(2*pi.*r_2.*b_2.*Bf_2));

    v_2t = (9.81.*11.42)./(240.855436775.*r_2);

    beta_2 = (atand(v_2n./(speed.*r_2-v_2t)))*(pi/180);

    outlet_blockage = 1 - ((n * t * b_2) / (2 * pi * r_2 * b_2 *
sin(beta_2)));

    if abs(Bf_2 - outlet_blockage) < 6e-4;

        v_2n = (Q./(2*pi.*r_2.*b_2.*Bf_2));

        v_2t = (9.81.*11.42)./(240.855436775.*r_2);

        beta_2 = (atand(v_2n./(speed.*r_2-v_2t)))*(pi/180);

        slip = 1 - ((sin(beta_2)).^(1/2))./(n.^0.7);

        v_2ts = slip.*v_2t;

        a = atand(v_2n./v_2ts);

        outflow_misalignment = 5.3 - a;

        outflow_list(n-4) = outflow_misalignment;

        velocity_mismatch = sqrt(((v_2ts).^2)+(v_2n).^2)-(Q/Area);

        velocity_list(n-4) = velocity_mismatch;

        outlet_blockagefactor(n-4) = Bf_2;

    end

end

end

outflow_list

```

```
k = 5:1:10;  
plot(k,outflow_list,'Linewidth',3)  
title('Angle Outflow Disalign vs Number of Blades')  
xlabel('Number of Blades')  
ylabel('Outflow Disalign [degrees]')  
grid on
```

```
figure()  
plot(k,velocity_list,'Linewidth',3)  
title('Velocity Mismatch vs Number of Blades')  
xlabel('Number of Blades')  
ylabel('Velocity Mismatch [m/s]')  
grid on
```

```
figure()  
plot(k,outlet_blockagefactor,'Linewidth',3)  
title('Outlet Blockage Factor vs Number of Blades')  
xlabel('Number of Blades')  
ylabel('Outlet Blockage Factor')  
grid on
```

```
figure()  
plot(k,inlet_blockagefactor,'Linewidth',3)  
title('Inlet Blockage Factor vs Number of Blades')  
xlabel('Number of Blades')  
ylabel('Inlet Blockage Factor')  
grid on
```